Geochimica et Cosmochimica Acta 365 (2024) 70–84

Contents lists available at ScienceDirect

Geochimica et Cosmochimica Acta

journal homepage: www.elsevier.com/locate/gca

Chlorine isotope evidence for Farallon-derived metasomatism of the North American lithospheric mantle

George Segee-Wright *, Jaime D. Barnes, John C. Lassiter

University of Texas at Austin, Department of Earth and Planetary Sciences, 2275 Speedway Stop C9000, Austin, TX 78712-0254, USA

ARTICLE INFO

Associate editor: Rosemary Hickey-Vargas

Keywords:
Chlorine isotopes
Lithosphere
Mantle
Subduction
Altered oceanic crust
HIMU

ABSTRACT

Metasomatism of the sub-continental lithospheric mantle (SCLM) can result in enrichment in volatile elements introduced via subduction of seawater-altered oceanic lithosphere. Subduction-related metasomatism can introduce chlorine isotope heterogeneity to the SCLM inherited from the subducted source, which can be used to characterize the source of metasomatism. This study presents Cl isotope compositions (δ^{37}Cl) of variably metasomatized continental lithospheric mantle xenoliths from the Colorado Plateau and southern Rio Grande Rift (southwestern United States). Fertile mantle xenoliths that represent asthenosphere that has recently been emplaced at the base of the North American lithosphere have δ^{37}Cl values of 0.0 ‰ to +0.1 ‰, suggesting that the convecting mantle has an average δ^{37}Cl value similar to seawater and chondrites. In contrast, metasomatized xenoliths span a range of δ^{37}Cl values from +0.1 ‰ to +1.9 ‰, extending above the average convecting mantle value. The range in δ^{37}Cl values can be explained by mixing between a subduction-related fluid with δ^{37}Cl values between +1.0 ‰ and +1.9 ‰ and a shallow crustal fluid with a δ^{37}Cl value less than +0.3 ‰. The most likely source of the high δ^{37}Cl subduction-related signature is the lower crust in the subducted Farallon plate. Lower crustal Cl likely entered the SCLM either through direct dehydration of lawsonite ± phengite in the deeply subducted Farallon plate or from a mixed serpentinite-oceanic crust source in the subducted Farallon. Regardless of the mechanism, this study provides evidence for subduction of crustal Cl into the mantle, which can introduce isotopic heterogeneity into the SCLM and has implications for the volatile cycling in the HIMU mantle and SCLM.

1. Introduction

Roughly 26 % and 30–32 % of Earth's Cl content is concentrated in the relatively small reservoirs of the ocean and lithosphere, respectively (e.g., Sharp and Draper, 2013; Kendrick et al., 2017). Low-temperature seawater alteration of the oceanic lithosphere results in large chlorine isotope fractionations, leading to a wide range of Cl isotope ratios (δ^{37}Cl values ≈ −2 to +2 ‰ vs SMOC) in altered oceanic crust and serpentinites (Barnes and Sharp, 2017 and references therein). In contrast, the depleted mantle has a low Cl concentration (<1 to 7 ppm; Bekaert et al., 2021; Kendrick et al., 2017; le Roux et al., 2006; Saal et al., 2002; Urann et al., 2020). The depleted mantle also has a relatively narrow range of δ^{37}Cl values, averaging −0.2 ± 0.5 ‰ (Selverstone and Sharp, 2011; Sharp et al., 2007, 2013). Although some authors suggest that the depleted mantle δ^{37}Cl value is lower (<−1.6 ‰; Bonifacie et al., 2008a; Layne et al., 2009), more recent work has suggested these lower values may be the result of analytical artifacts (Sharp et al., 2013). These mantle estimates are largely based on analyses of MORB glasses, and some other mantle-derived materials, such as mantle halite and inclusions in fibrous diamonds. To our knowledge, there are no published chlorine isotope data on unaltered mantle peridotite xenoliths. However, there is one published value of a metasomatized SCLM xenolith from Greenland (δ^{37}Cl value=+1.3 ‰; Hoare et al., 2021) and published data on alpine peridotites from Balmuccia and Finero (Ivrea Zone, Italy) (δ^{37}Cl value = −1.8 ‰ to +2.1 ‰; Selverstone and Sharp, 2011). Due to the contrasting Cl concentrations and δ^{37}Cl values of the depleted mantle (<7 ppm; Bekaert et al., 2021) and altered lithosphere (100′s-1000′s ppm; e.g. Barnes and Sharp, 2017), the mobility of Cl in aqueous fluids, and the lack of significant Cl isotope fractionation during high temperature processes (Balan et al., 2019; Schauble et al., 2003), chlorine isotope ratios have been used as a tracer of different slab-derived fluids in arc lavas and volcanic gases (e.g., Barnes et al., 2008, 2009a; Barnes and Straub, 2010; Chiaradia et al., 2014; Bouvier et al., 2019, 2022a, 2022b; Liotta et al., 2017; Manzini et al., 2017). Such studies have found large deviations from depleted mantle δ^{37}Cl values at arc settings due to dehydration of subducted lithosphere.

* Corresponding author.
E-mail address: ghs562@utexas.edu (G. Segee-Wright).

https://doi.org/10.1016/j.gca.2023.11.030
Received 24 July 2023; Accepted 28 November 2023
Available online 1 December 2023

However, Cl isotope variations have not been well studied in subduction-modified SCLM in non-arc settings.

Slab-derived fluids or melts can be introduced to the SCLM (e.g., Broadley et al., 2016). The Cl isotope composition of subduction-modified SCLM can elucidate the source and quantity of subducted volatiles in areas without arc magmatism, expanding our understanding of volatile cycling into the mantle. The SCLM is frequently sampled by intracontinental volcanic zones as basaltic melts and peridotite and pyroxenite xenoliths. Though intra-continental basalts are common, they often suffer from shallow degassing of Cl as HCl, which can isotopically fractionate Cl (Sharp et al., 2010; Barnes et al., 2014b; Fischer et al., 2015; Liotta et al., 2017). To avoid such fractionation, only material that has not undergone extensive degassing at pressures lower than 4–25 MPa (Unni and Schilling, 1978; Lesne et al., 2011) are likely to accurately represent the δ^{37}Cl value of the SCLM from which it is derived. These constraints limit the potential source of unfractionated, SCLM-derived Cl to melt inclusions and SCLM xenoliths.

Currently, there are no published δ^{37}Cl values from intraplate melt inclusions and only one analysis of δ^{37}Cl values of an SCLM xenolith from Greenland (Hoare et al., 2021). Here we report bulk δ^{37}Cl values, in addition to bulk [H_2O], bulk hydrogen isotope ratios (δD), and clinopyroxene oxygen isotope ratios ($\delta^{18}O_{cpx}$), of 28 modally hydrated lithospheric mantle xenoliths from the Navajo Volcanic Field (New Mexico, United States), one anhydrous refractory peridotite xenolith from Elephant Butte (New Mexico, United States), and two anhydrous fertile peridotite xenoliths from Elephant Butte.

2. Geological setting and samples

2.1. Navajo Volcanic Field and the Colorado Plateau

Hydrous-mineral-bearing SCLM xenoliths in this study come from the Navajo Volcanic Field in the central Colorado Plateau. The Colorado Plateau is a relatively stable block of lithosphere characterized by thick crust (42–55 km) and lithosphere (>120–150 km) (Gao et al., 2004; West et al., 2004). The Navajo Volcanic Field is composed of ~50 minette necks and ~8 diatreme-forming serpentinized ultramafic microbreccia (SUM) intrusions that formed at 30–24 Ma (Roden, 1981; Smith, 1979, 2010; Smith et al., 2004). Minettes and SUM diatremes commonly host a variety of xenoliths including peridotite, pyroxenite, eclogite, and metasedimentary rocks (e.g., Selverstone et al., 1999). The SUM diatremes erupted as solid–gas mixtures (McGetchin et al., 1973; Smith and Levy, 1976; Smith, 1995) with eruptive temperatures <530–650 °C (Smith, 2013). While the SUM diatremes are temporally and spatially related to minettes, the SUM diatremes were not derived from silicate melts but rather were likely formed from the intrusion of minette magmas into the hydrated SCLM (Smith and Levy, 1976).

The Navajo Volcanic Field occurs along the suture between the Yavapai and Mazatzal crustal provinces with minettes and SUM diatremes on both sides of the suture (Fig. 1; Bennett and DePaolo, 1987; Karlstrom and Bowring, 1993, Selverstone et al., 1999). Based on differing P-T histories, alteration records, deformation records, and xenolith populations across the suture, Selverstone et al. (1999) proposed that the suture results from a northwest dipping Proterozoic paleo-subduction zone with the Yavapai and Mazatzal crustal provinces composing the overriding and subducting plates, respectively.

Evidence from fluid-mobile element enrichment (Lee, 2005), mineral chemistry and petrography (Smith, 1979, 1995, 2010), and stable isotope ratios (Perkins et al., 2006; Marshall et al., 2017b) indicate that the SCLM beneath the Colorado Plateau was metasomatized by aqueous fluids (e.g., Roden et al., 1990; Marshall et al., 2017b; Segee-Wright et al., 2023) or carbonated/hydrous melts (Lee, 2005; Perkins et al., 2006). Sm-Nd, Rb-Sr and U-Pb ages in hydrated/metasomatized xenoliths (Smith et al., 2004; Lee, 2005; Marshall et al., 2017a), trace element zonation in discrete SUM-hosted garnet grains (Smith, 2020), Fe-Mg gradients in mantle xenoliths (Smith, 1979), and inter-mineral

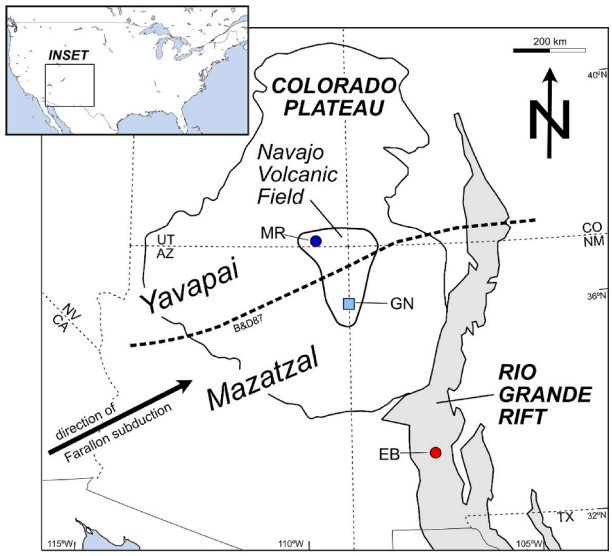

Fig. 1. Map of the Colorado Plateau and Rio Grande Rift and the xenolith localities from which samples in this study were collected. MR = Moses Rock; GN = Green Knobs; EB = Elephant Butte. Dashed line is the preferred suture between the Yavapai and Mazatzal provinces from Selverstone et al. (1999). BD87= Bennett and DePaolo (1987). After Selverstone et al. (1999) and Hudson and Grauch (2013).

oxygen isotope disequilibria (Perkins et al., 2006) suggest that metasomatism of the Colorado Plateau SCLM occurred <25 million years before emplacement of xenoliths and is likely related to the subducted Farallon plate while it was undergoing shallow-slab subduction at ~80–40 Ma, not from earlier Proterozoic subduction.

Both the ultimate source of the Farallon-related metasomatic fluid and the extent of SCLM hydration/metasomatism are debated. Previous studies have suggested dehydration of the serpentinized oceanic mantle in the subducted Farallon plate (Lee, 2005; Li et al., 2008; Marshall et al., 2017b), melting of the subducted Farallon crust and carbonated sediments (Lee, 2005; Perkins et al., 2006), and tectonically eroded Mojave forearc mantle (Smith, 2010, 2020) as potential metasomatizing agents. Additionally, several studies have suggested that hydration/metasomatism of the North American SCLM is laterally extensive, extending across much of the Colorado Plateau and Rio Grande Rift (Lee, 2005; Perkins et al., 2006; Li et al., 2008; Segee-Wright et al., 2023) and possibly contributing to the uplift of the western US (Humphreys et al., 2003). However, other studies suggest more localized hydration/metasomatism of the SCLM beneath the Navajo Volcanic Field due to fluid/diapir flow along monoclines (Smith et al., 2010, 2020). The Navajo Volcanic Field was >700 km from the convergent boundary between the Farallon and North American plates. The mechanism for retention of hydrous minerals in the Farallon plate to these great distances is uncertain but is likely related to the fast plate motion (10–15 cm/year; English, 2003), its contact with the relatively cool North American SCLM, and the potential subduction of a thick oceanic plateau (e.g. Livaccari et al., 1981, Liu et al., 2008), all of which may have delayed conductive heat flow into the subducting Farallon plate and allowed for the retention of hydrous mineral in the subducted plate at great distances from the trench.

Navajo Volcanic Field samples in this study are SUM-hosted SCLM peridotite xenoliths from Green Knobs (n = 25) and Moses Rock (n = 3) sampling SCLM from both sides of the Yavapai-Mazatzal suture (Fig. 1). The same xenoliths from this study have been previously analyzed for Re-Os and geothermometry. The xenoliths have Re depletion ages of 1.7 to 2.1 Ga (Marshall et al., 2017a), consistent with the age of the overlying Yavapai-Mazatzal terrane (Anderson and Morrison, 2005) and similar to ages of other Colorado Plateau SCLM xenoliths (Lee et al.,

2001; Byerly and Lassiter, 2012). Thermometry studies of these xenoliths report conflicting temperature conditions spanning >450 °C in a single xenolith depending on the geothermometer used. However, a compilation of xenolith temperature calculations by Behr and Smith (2016) indicates that all xenoliths are samples of the mantle that cooled to below 700–800 °C, and higher temperatures calculated from two-pyroxene geothermometers resulted from lack of equilibration to lower temperature conditions in undeformed peridotite.

Most Navajo Volcanic Field xenoliths are hydrated spinel lherzolites, though two samples (N23-GN, N71-GN) contain chlorite pseudomorphs of garnet (Roden et al., 1990) and two samples (EMGN21 and EMGN24) contain clinopyroxene rare earth element patterns that suggest previous presence of garnet (Roden and Shimizu, 1993; Marshall et al., 2017a). Samples contain <5 to 95 modal % hydrous minerals. Xenoliths contain two generations of hydrous minerals: early-stage hydrous minerals (antigorite, chlorite, amphibole, and minor titanoclinohumite and phlogopite) that formed at depth in the lithospheric mantle prior to SUM eruption (Smith, 1979,2010; Marshall et al., 2017b), and late-stage hydrous minerals (lizardite/chrysotile) that fill fractures and likely formed *syn*-emplacement (Segee-Wright et al., 2023). For additional petrographic details and photomicrographs, see Marshall et al., (2017a), Segee-Wright et al., 2023, Roden et al. (1990), Smith (2010), and Behr and Smith (2016).

Marshall et al., (2017b) measured high hydrogen isotope ratios (δD values = −79 ‰ to –33 ‰) in early-stage hydrous minerals, consistent with a subduction-derived origin of the metasomatic fluid (e.g., Shaw et al., 2008). Marshall et al., (2017b) also observed a negative correlation between olivine oxygen isotope ratios ($\delta^{18}O_{olv}$) and cpx trace element ratios (Ce/Sm, La/Sm), which were attributed to interaction of the SCLM with a low-$\delta^{18}O$ metasomatic fluid from the subducted Farallon plate. Segee-Wright et al. (2023) measured halogen (F, Cl, Br, and I) bulk rock concentrations in these xenoliths. They observed highly elevated Cl and Br contents that correlated with $\delta^{18}O_{olv}$, but little or no F enrichment, which they attributed to halogen enrichment from dehydration of subducted sub-crustal serpentinite or from altered oceanic crust in the Farallon plate. However, the similarity of the halogen signatures of these potential metasomatic source makes it difficult to differentiate between them. Most Navajo Volcanic Field xenoliths in this study have also been characterized for mineral and bulk major, minor, and trace element compositions. For additional information on these samples, see Behr and Smith (2016), Marshall et al. (2018), Marshall et al., (2017a, 2017b), Smith (1979, 2010, 2013, 2020), Smith and Levy (1976), and West et al. (2004).

2.2. Elephant Butte

Elephant Butte is in the southern Rio Grande Rift (Fig. 1). The rift stretches from Colorado to northern Mexico (Fig. 1; Keller et al., 1991). Rifting began at 36 Ma to 27 Ma (Chapin, 1979; Mack et al., 1994), possibly associated with a shift from a compressional to extensional stress regime during rollback of the Farallon slab following the Laramide orogeny (Humphreys, 1995; Lawton and McMillan, 1999). After early volcanism associated with rifting, there was a period of volcanic quiescence in the Miocene followed by a shift in the composition of erupted lavas after 10 Ma towards more depleted Sr and Nd isotopic compositions (Baldridge et al., 1980; McMillan et al., 2000). This shift is likely associated with a shift from lithospheric to asthenospheric mantle melting after removal of the lower SCLM beneath the southern Rio Grande Rift and replacement with asthenosphere (McMillan et al., 2000; Byerly and Lassiter, 2012). This is consistent with the relatively thin (45–55 km) lithosphere and slow seismic velocities beneath the Rio Grande Rift (Gao et al., 2004; West et al., 2004; Wilson et al., 2005).

Elephant Butte consists of cinder cones and lava flows that formed during or after the Pliocene along the southern Rio Grande Rift (Baldridge et al., 1980) and contains basalt- and trachybasalt-hosted spinel lherzolite xenoliths. All Elephant Butte xenoliths are protogranular or equigranular with coarse grain sizes (olivine 0.5–8 mm) (Byerly and Lassiter, 2012). All xenoliths in this study are categorized as Group I xenoliths following the classification scheme of Frey and Prinz (1978) with Cr-rich spinel and clinopyroxene (Byerly and Lassiter, 2012). The xenoliths are divided into refractory and fertile xenoliths. Refractory xenoliths have been interpreted as Proterozoic lithospheric mantle based on their high spinel Cr# (0.15–0.5), low bulk rock Al_2O_3 (0.65–2.29 wt%), low cpx Yb (0.14–1.42 ppm), low cpx modal abundance, and rare earth element and radiogenic isotope patterns similar to refractory but metasomatized SCLM from the Colorado Plateau (Byerly and Lassiter, 2012). Fertile xenoliths are interpreted as asthenospheric mantle recently emplaced at the base of the lithosphere after partial delamination of the Proterozoic SCLM based on low spinel Cr# (0.06–0.21), depleted-mantle-like bulk Al_2O_3 (3.3–4.6 wt%), high cpx Yb (1.7–2.2 ppm), Os isotope compositions similar to abyssal peridotites, and Sr and Nd isotope compositions that are much more depleted than the nearby Colorado Plateau SCLM and extend the depleted end of the MORB Sr-Nd trend (Byerly and Lassiter, 2012). Although fertile Elephant Butte xenoliths retain chemical signatures of the convecting upper mantle, they are not direct samples of the asthenosphere but rather were physically part of the SCLM prior to eruption and likely equilibrated at shallower depths (~40–45 km) than the lithosphere-asthenosphere boundary (Byerly and Lassiter, 2012).

All Elephant Butte xenoliths presented in this study have been previously characterized for bulk rock halogen content (F, Cl, Br, and I; Segee-Wright et al., 2023), and most have been characterized for bulk rock major, minor, trace element, and radiogenic isotope compositions (Byerly and Lassiter, 2012).

3. Methods

The extraction and measurement of chlorine isotope ratios were conducted at the University of Texas at Austin (UT Austin) using the method outlined by Eggenkamp (1994) and Magenheim et al. (1994), as modified by Barnes and Sharp (2006) and Sharp et al. (2007). Interior sections of xenoliths with no visible alteration were powdered and cleaned with 18.2 MΩ water to remove surficial halogen contamination and dried at 40 °C for two days. Dried powders were mixed with 99.99 % pure vanadium pentoxide flux. Chloride was extracted via pyrohydrolysis into an aqueous solution, reacted with $AgNO_3$ to precipitate AgCl, and reacted with CH_3I to form CH_3Cl. CH_3Cl was then purified of excess CH_3I in a gas chromatography column in a continuous He flow. The CH_3Cl isotope composition was then analyzed on a ThermoElectron MAT 253. Data are reported in standard per mil notation versus standard mean ocean chloride (‰ vs SMOC). The average standard deviation is ± 0.2 ‰ (1SD) based on long-term reproducibility of seawater standard measurements. The errors associated with sample duplicates fall within this standard deviation, suggesting the error on unknowns is associated with the isotope measurements, not with sample preparation.

To avoid potential analytical error associated with analyzing samples with low Cl contents (<20 μg total Cl; Sharp et al., 2013), multiple splits of low [Cl] samples (Elephant Butte samples) underwent pyrohydrolysis. The resulting aqueous solutions from the different splits were each analyzed for Cl concentration using a Dionex ICS 2000 Ion Chromatograph at UT Austin. Given the Cl concentration in the aqueous solution, the volume of solution, and the mass of sample pyrohydrolyzed, one can calculate the Cl concentration in the bulk rock. For all three low-Cl samples, calculated Cl concentrations of the bulk rock powders were identical within 0.5 ppm for all splits of a given sample. The uniformity of the different splits indicates that no Cl contamination occurred during pyrohydrolysis. The different aqueous solutions for each sample were then combined to form solutions with >30 μg Cl, which were then analyzed for their Cl isotope ratio.

Clinopyroxene $\delta^{18}O$ ($\delta^{18}O_{cpx}$) values were measured using the laser fluorination method of Sharp (1990) at UT Austin with a ThermoElectron MAT 253. Approximately 2.5 mg of optically clear

Table 1
Average Chemical and Isotopic Data.

Sample Name	Locality	Xenolith source	δD bulk (‰ vs VSMOW)	± (2SE)	δ^{37}Cl bulk (‰ vs SMOC)	± (2SE)	$\delta^{18}O_{cpx}$(‰ vs VSMOW)	± (2SE)	Bulk Water (wt%)	± (2SE)
Anhydrous peridotites										
BELB9-6	EB-F	AM			0.1		5.16	0.03		
BELB9-8	EB-F	AM			0.0		4.99	0.17		
BELB9-15	EB-R	SCLM			1.2		5.26	0.01		
Modally hydrated peridotites										
EMGN10	NVF-GN	SCLM	−58	0.7	1.0				6.7	0.06
EMGN12	NVF-GN	SCLM	−64	1.0	1.7				5.1	0.06
EMGN14	NVF-GN	SCLM	−71	0.5	0.4				4.6	0.02
EMGN17	NVF-GN	SCLM	−98	1.1	0.6				4.0	0.02
EMGN2	NVF-GN	SCLM	−101	0.5	1.2				1.3	0.01
EMGN21	NVF-GN	SCLM	−65	0.2	1.7				4.4	0.01
EMGN23	NVF-GN	SCLM			1.2				4.0	
EMGN24	NVF-GN	SCLM	−53	0.3	1.0				5.7	0.02
EMGN26	NVF-GN	SCLM	−117	0.9	−0.1		5.33	0.06	2.6	0.01
EMGN27	NVF-GN	SCLM	−84	0.8	0.5				4.5	0.08
EMGN29	NVF-GN	SCLM	−85	0.3	0.7				2.4	0.03
EMGN7	NVF-GN	SCLM	−80	0.2	1.2				3.0	0.00
EMGN9	NVF-GN	SCLM	−64	0.5	1.0	0.3			5.6	0.04
N106-GN	NVF-GN	SCLM	−87	1.0	0.8		5.14		1.4	0.05
N126-GN	NVF-GN	SCLM	−106	0.7	0.4	0.1	5.39	0.22	2.4	0.02
N15-GN	NVF-GN	SCLM	−51	0.8	0.9				9.0	0.17
N16-GN	NVF-GN	SCLM	−104	0.6	0.9		5.21	0.18	2.1	0.01
N178-GN	NVF-GN	SCLM	−88	0.6	1.7		5.06		2.6	0.03
N17-GN	NVF-GN	SCLM	−86	0.3	1.4		5.21		1.7	0.01
N23-GN	NVF-GN	SCLM	−48	0.0	1.9				5.1	0.02
N51-GN	NVF-GN	SCLM	−84	0.1	1.0	0.1			4.5	0.01
N55-GN	NVF-GN	SCLM	−77	0.1	0.8		5.32		1.7	0.04
N57-GN	NVF-GN	SCLM	−69	0.9	0.9				2.6	0.03
N61-GN	NVF-GN	SCLM	−106	1.6	0.5		5.24		1.0	0.02
N71-GN	NVF-GN	SCLM	−79	0.3	1.6				4.9	0.10
EMMR4	NVF-MR	SCLM	−84	0.3	1.6	0.3			10.6	0.05
EMMR7	NVF-MR	SCLM	−122	0.4	1.1				3.6	0.07
MR-ATG-13	NVF-MR	SCLM	−111	1.5	0.9		5.23	0.14	3.0	0.04

AM: Asthenospheric Mantle, SCLM: Sub-Continental Lithospheric Mantle. EB-F: Fertile Elephant Butte, EB-R: Refractory Elephant Butte, NVF-GN: Navajo Volcanic Field- Green Knobs, NVF-MR: Navajo Volcanic Field-Moses Rock. 2SE = Two times the standard error.

clinopyroxene were hand-picked under a transmitted light binocular microscope. Samples were analyzed 1–3 times. Garnet standard UWG-2 ($\delta^{18}O = +5.8$ ‰; Valley et al., 1995), in-house olivine standard San Carlos ($\delta^{18}O = +5.3$ ‰), and in-house quartz standard Lausanne-1 ($\delta^{18}O = +18.1$ ‰) were analyzed to determine accuracy and precision. All $\delta^{18}O$ values are reported in standard per mil notation relative to VSMOW. Error on long-term analysis of standards is < 0.1 ‰ (1SD) and replicates of in-run standards is < 0.03 ‰ (1SD).

Bulk rock δD and [H_2O] values were determined using the methods of Sharp et al. (2001) at UT Austin using a ThermoElectron MAT 253 mass spectrometer. 2.5–12 mg of bulk rock powder was loaded into silver capsules, which were pyrolyzed in a ThermoElectron MAT high temperature conversion elemental analyzer (TC-EA). Analyses of USGS-57, USGS-58, IAEA-CH7, and NBS-22 were used to construct a δD calibration curve, and analyses of USGS-57 and USGS-58 were used to construct a [H_2O] calibration curve. All δD values are reported in standard per mil notation relative to SMOW. Average external error on each δD analysis is <5 ‰ and on water content is <0.1 wt%. Hydrogen isotope measurements are not reported on the Elephant Butte samples due to low water contents in the samples.

Modal abundances of different early-stage hydrous minerals were determined for a subset of samples via point counting on a thin section using a petrographic microscope and BSE and EDS element maps acquired using a JEOL JSM 6490LV Scanning Electron microscope at UT Austin (see Segee-Wright et al., 2023). These modal abundances were then used to estimate the proportion of water in the xenoliths from early-stage and late-stage hydrous minerals. Due to the small scale of the late-stage fracture-filling serpentine, modal abundances were not collected for the late-stage serpentine. Instead, the difference between the total water content measured in the xenolith (from TC-EA) and the early-stage water content was assumed to be in the late-stage serpentine. For these calculations, water contents and densities of amphibole, chlorite, serpentine, and clinohumite were assumed to be ~2.5 wt% and ~3.0 g/cm^3, ~13 wt% and ~2.65 g/cm^3, ~12.5 wt% and ~2.55 g/cm^3, ~2 wt% and ~3.26 g/cm^3, respectively. The water contents are based on previously analyzed mineral compositions of hydrous minerals from Navajo Volcanic Field xenoliths from Smith (2010). Density estimates are based on values from Hacker et al. (2003). See supplementary material for hydrous mineral modal abundances.

4. Results

All δ^{37}Cl, $\delta^{18}O$, and δD values are shown in Table 1. Chlorine isotope ratios of the Navajo Volcanic Field xenoliths range from +0.1 ‰ to +1.9 ‰, extending to higher than the typical range of convecting mantle δ^{37}Cl values (−0.2 ± 0.5; Fig. 2). Chlorine isotope ratios do not correlate strongly with [Cl] or Cl/Nb (Cl concentrations given in Table S2 in Appendix A; Segee-Wright et al., 2023) in these xenoliths (Fig. 3) but form a positive correlation with bulk rock δD (Fig. 4). This correlation is statistically significant with a non-directional p-value of 0.011. The refractory SCLM xenolith from Elephant Butte has a δ^{37}Cl value of +1.2 ‰, whereas the two fertile xenoliths have δ^{37}Cl values of 0.0 ‰ and +0.1 ‰.

SCLM xenoliths from Navajo Volcanic Field and Elephant Butte have $\delta^{18}O_{cpx}$ values that range from 5.06 to 5.50 ‰, extending to values lower than typical mantle $\delta^{18}O_{cpx}$ (5.25 to 5.89 ‰; Mattey et al., 1994). These $\delta^{18}O_{cpx}$ data correlate negatively with early-stage hydrous mineral

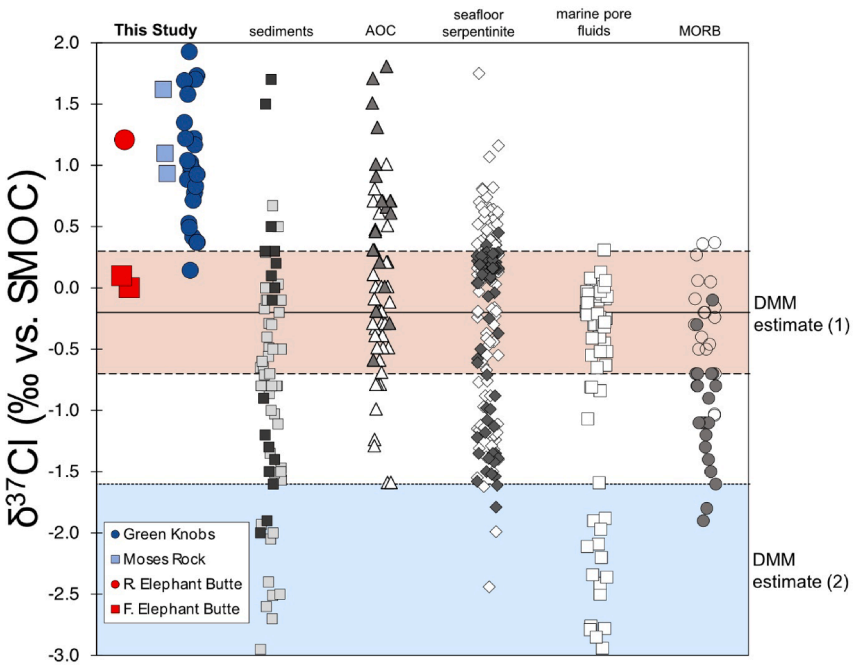

Fig. 2. Cl isotope data from this study and from various subducted materials and MORB. AOC = altered oceanic crust. MORB = mid-ocean ridge basalt. DMM = depleted MORB-source mantle. Green Knobs and Moses Rock are localities in the Navajo Volcanic Field. R. Elephant Butte = Refractory Elephant Butte. F. Elephant Butte = Fertile Elephant Butte. Gray and black squares are marine and non-marine sediments, respectively. White and gray triangles are low-temperature and high-temperature altered oceanic crust, respectively. White and gray diamonds are structurally bound and water-soluble Cl fractions in seafloor serpentinite, respectively. Open and filled circles for MORB data come from Sharp et al. (2007) and Bonifacie et al., (2008a), respectively. DMM estimate (1) is from Sharp et al. (2007). DMM estimate (2) is from Bonifacie et al., (2008a) and Layne et al. (2009). Fertile Elephant Butte samples fall within the range of DMM estimate (1), not (2). Data sources: porewaters: Ransom et al. (1995), Hesse et al. (2000), Godon et al. (2004), Bonifacie et al. (2007); sediments: 2009a,2009b);Barnes et al., (2008, (Selverstone and Sharp (2015); altered oceanic crust: Barnes and Cisneros (2012); serpentinites: Barnes and Sharp (2006), Bonifacie et al., (2008b), Barnes et al., (2008,2009a,2009b).

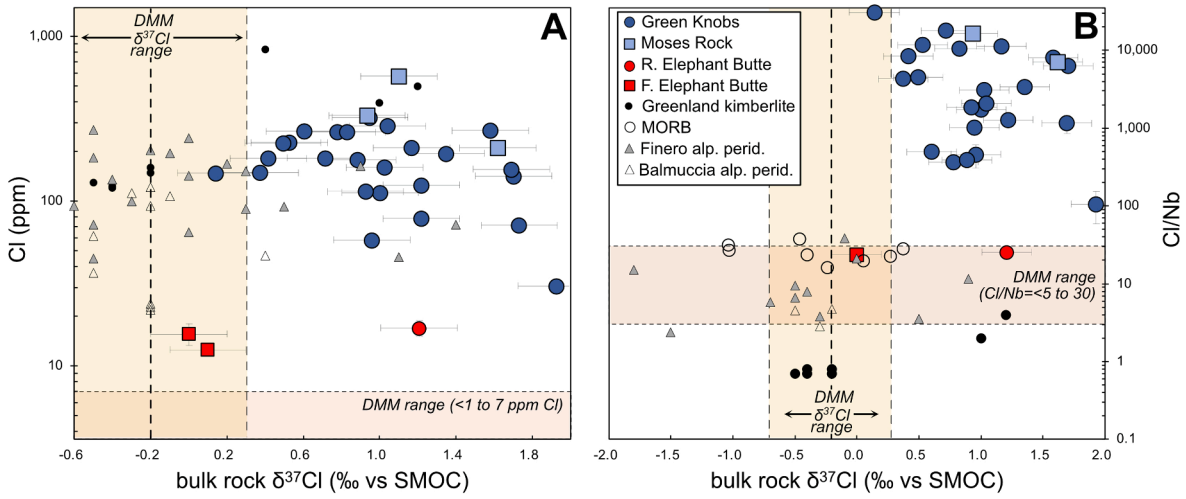

Fig. 3. (A) Bulk rock Cl concentrations and (b) bulk rock Cl/Nb in xenoliths vs the bulk rock δ^{37}Cl values. R. Elephant Butte = Refractory Elephant Butte; F. Elephant Butte = Fertile Elephant Butte; alp. perid. = alpine peridotite; DMM = depleted MORB-source mantle. There is little or no correlation between Cl or Cl/Nb and δ^{37}Cl values. Xenolith Cl concentration data from Segee-Wright et al. (2023). Xenolith [Nb] data from Marshall et al., (2017a) and Byerly and Lassiter (2012). MORB [Cl] and δ^{37}Cl data from Sharp et al. (2007). MORB [Nb] data from PetDB database (www.earthchem.org/petdb; see supplementary material for individual references). Kimberlite [Cl] and δ^{37}Cl data from Hoare et al. (2021). Alpine peridotite data from Selverstone and Sharp (2011). DMM [Cl] and Cl/Nb estimates based on Kendrick et al. (2017), Bekaert et al. (2021), and Saal et al. (2002). The range (1 SD) of DMM δ^{37}Cl values from Sharp et al. (2007). Error bars are 1SD.

modal abundance (non-directional p-value = 0.024; Fig. 5a) and bulk rock δ^{37}Cl values (non-directional p-value = 0.005; Fig. 5b). The two fertile xenoliths from Elephant Butte have $\delta^{18}O_{cpx}$ values of 4.99 ‰ and 5.16 ‰ and do not fall along the δ^{37}Cl-$\delta^{18}O_{cpx}$ trend defined by the lithospheric xenoliths (Fig. 5b).

Bulk xenolith δD values range from −48 ‰ to −122 ‰ and correlate positively with the proportion of early- to late-stage hydrous minerals (non-direction p-value < 0.0001; Fig. 6). Samples where late-stage serpentine makes up >90 % of the hydrous minerals have δD values ranging from −122 ‰ to −101 ‰, whereas samples in which late-stage serpentine makes up <30 % of the hydrous minerals have δD values ranging from −84 ‰ to −48 ‰.

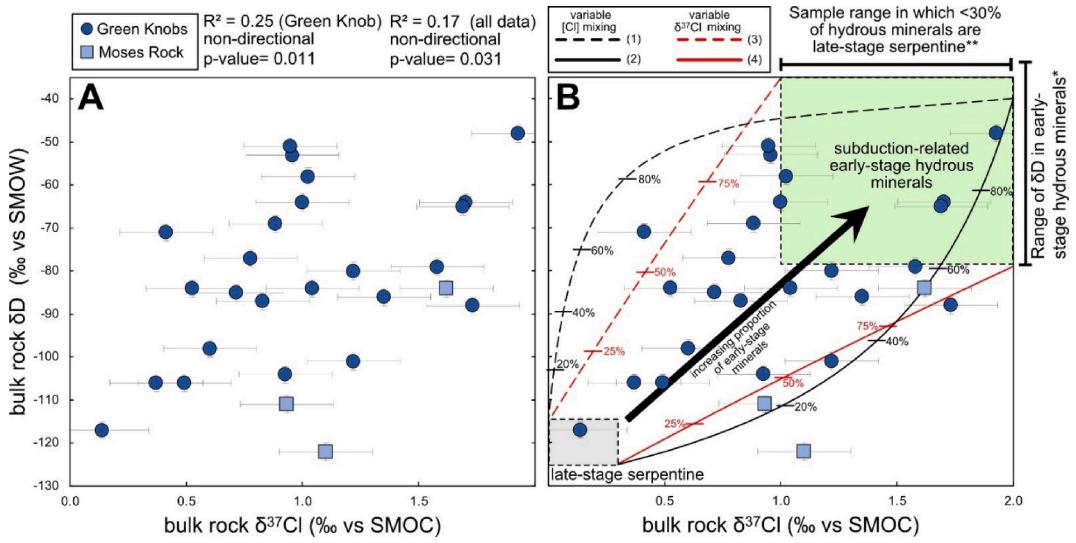

Fig. 4. Bulk Chlorine isotope ratios plotted against the bulk hydrogen isotope ratios in Navajo Volcanic Field samples from Green Knobs and Moses Rock. The gray box indicates a hypothetical range of $\delta^{37}Cl$ and δD values for late-stage serpentine at Green Knobs based on $\delta^{37}Cl$ and δD values of samples with no early-stage hydrous minerals (see Section 5.2 of text). This range is not applied to Moses Rock because the two localities are ~140 km from one another which could result in different interactions with shallow crustal fluids. The green box is a range of possible $\delta^{37}Cl$ and δD values for early-stage hydrous minerals based on $\delta^{37}Cl$ values of xenoliths with >70 % early-stage hydrous minerals and δD values of early-stage hydrous mineral separates from Marshall et al., (2017b). The black and red curves are mixing arrays between late-stage serpentine and early-stage hydrous minerals with varying [Cl] (black) and $\delta^{37}Cl$ (red) of the two components. See supplementary material for mixing array details. *Data from Marshall et al., (2017b). **<30 % of the hydrous minerals in the xenolith are late-stage serpentine.

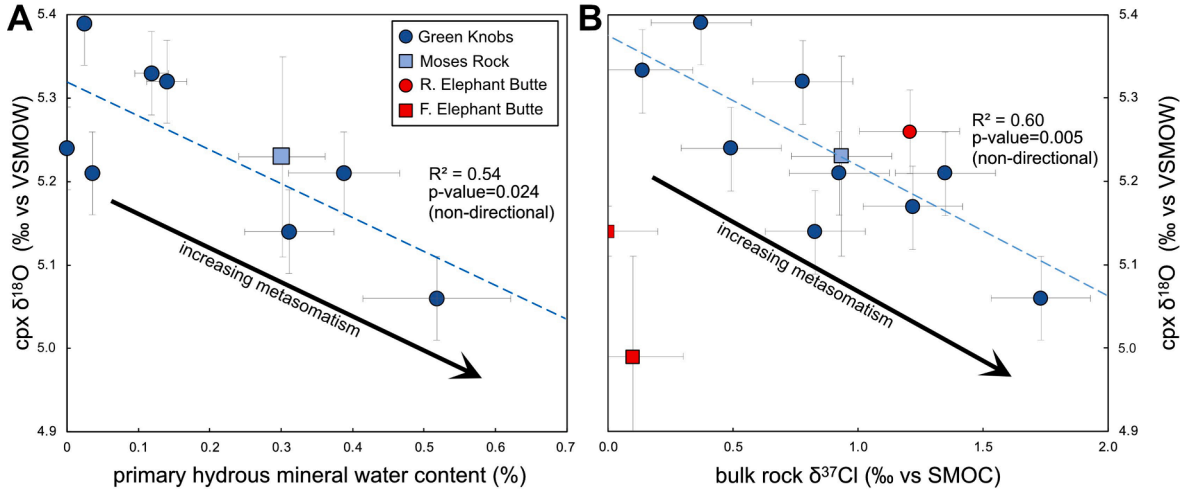

Fig. 5. Clinopyroxene oxygen isotope ratios plotted against (A) calculated bulk primary hydrous water content and (B) bulk rock $\delta^{37}Cl$ values. Primary hydrous water content is calculated using the assumptions outlined in Section 3 (Methods). Error bars are either 1 SD of standards or of sample duplicates, whichever was larger. Increasing $\delta^{37}Cl$ values and decreasing $\delta^{18}O_{cpx}$ values are interpreted as increased subduction-related metasomatism of the SCLM. R. Elephant Butte = Refractory Elephant Butte. F. Elephant Butte = Refractory Elephant Butte. Fertile Elephant Butte samples (gray squares) do not plot along this array because they were not part of the SCLM until recently.

5. Discussion

5.1. Depleted mantle chlorine isotope composition

While $\delta^{37}Cl$ values of MORB glasses have previously been used as proxies for the $\delta^{37}Cl$ value of the depleted mantle, chlorine isotope ratios in fertile peridotite xenoliths from Elephant Butte in this study can provide another line of evidence for the $\delta^{37}Cl$ composition of the depleted mantle. The $\delta^{37}Cl$ composition and degree of isotopic heterogeneity of Earth's mantle has implications for the primordial Earth's volatile element content and the subduction of volatiles into the mantle. Several studies suggest that the depleted mantle has a homogenous seawater-like $\delta^{37}Cl$ composition (-0.2 ± 0.5 ‰; Fig. 2; Sharp et al., 2007, 2013; Selverstone and Sharp, 2011). However, other studies indicate that the depleted mantle has a value of −1.6 ‰ to −3‰ and suggest values closer to 0 ‰ are the result of seawater contamination (Fig. 2; Bonifacie et al., 2008a; Layne et al., 2009). This disagreement results in a ~3 ‰ range for $\delta^{37}Cl$ estimates of the average convecting mantle, spanning most of the range of $\delta^{37}Cl$ values observed on Earth and complicating conclusions about the quantity and source of subducted Cl at both arc and non-arc settings.

All previous depleted mantle $\delta^{37}Cl$ estimates used data from MORB glasses, alpine peridotites, and rare high-Cl mantle minerals (Sharp et al., 2007, 2013; Bonifacie et al 2008a, 2008b; Selverstone and Sharp, 2011), all of which can be altered by seawater/brine assimilation or late metamorphism/metasomatism and may not be representative material

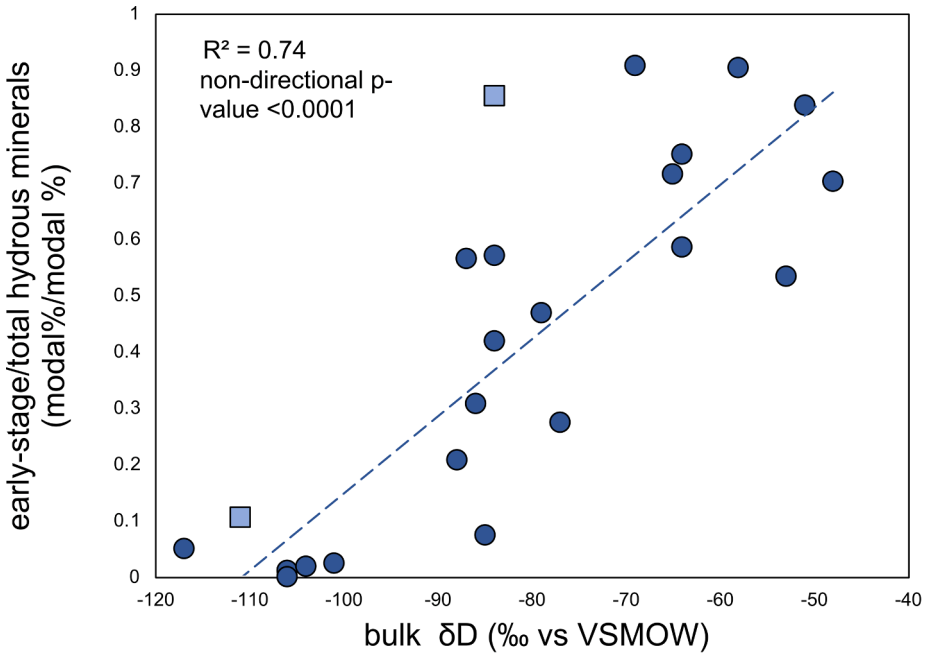

Fig. 6. Bulk rock δD values plotted against early-stage hydrous minerals relative to the total hydrous minerals. A higher δD value at higher fractions of early-stage hydrous minerals suggests that the range of δD values results from mixing of early-stage hydrous minerals formed through interaction with subduction-related fluids and late-stage serpentine formed through interaction with shallow crustal fluids.

for the average convecting mantle. However, the two fertile peridotite xenoliths from Elephant Butte have LREE depletions and depleted MORB-like radiogenic isotope compositions that suggest they were recently part of the convecting mantle (Byerly and Lassiter, 2012). As such, these fertile xenoliths are a more direct representation of the asthenospheric mantle δ^{37}Cl value.

The Cl concentrations of these fertile xenoliths (12–15 ppm; Fig. 3a) are slightly higher than the accepted range of Cl concentrations in the convecting mantle (<1–7 ppm; Saal et al., 2002; Kendrick et al., 2017). However, the samples have bulk Cl/Nb (~24; Fig. 3b) consistent with uncontaminated MORB (Kendrick et al., 2017) and lower Cl concentration than in any alpine peridotite previously analyzed for δ^{37}Cl (Fig. 3a; Selverstone and Sharp, 2011). While we cannot completely rule out the possibility that the slightly elevated Cl contents in these xenoliths reflect interaction with a late-stage fluid similar to that observed in Navajo Volcanic Field samples (see Section 5.2), the depleted mantle-like Cl/Nb values make that unlikely. The fertile Elephant Butte Cl/Nb are significantly lower than other xenoliths interpreted to have a have interacted with late-stage fluid (see section 5.2; bulk Cl > 100 ppm and Cl/Nb > 100; Fig. 3b), inconsistent with late-stage addition of Cl from fluids that would be characterized by high Cl/Nb.

A more likely explanation for the elevated Cl but depleted mantle-like Cl/Nb is melt metasomatism. However, the depleted, MORB-like radiogenic isotope compositions of these xenoliths (Byerly and Lassiter, 2012) suggest the fertile Elephant Butte samples have not interacted with a subduction-derived melt. Interaction with a melt derived from subducted crust or sediments could result in the observed elevated Cl and incompatible trace element concentrations but would also result in more radiogenic Sr than is observed ($^{87}Sr/^{86}Sr = 0.70227$; Byerly and Lassiter, 2012). Instead, the fertile Elephant Butte xenolith compositions likely reflect either metasomatism from their basaltic hosts during eruption or from melt interaction prior to eruption. However, the source of the young Pliocene host basalts is thought to be recently emplaced asthenosphere (McMillan et al., 2000). Because this is the same source as the fertile Elephant Butte xenoliths, the host basalt will likely have the same δ^{37}Cl value as the fertile Elephant Butte xenoliths. Equilibration temperatures of the fertile Elephant Butte xenoliths are 1015 ± 15 °C (Byerly and Lassiter, 2012), at which temperatures little isotope fractionation will occur during melt metasomatism of these xenoliths (Balan et al., 2019). Therefore, while some degree of autometasomatism may have occurred in these xenoliths, the near-zero δ^{37}Cl values of these xenoliths (average δ^{37}Cl = +0.05 ‰) suggest that average asthenospheric mantle has a δ^{37}Cl value of ~0 ‰, consistent with the depleted mantle estimate of Sharp et al. (2007) and with the composition of chondrites (Sharp et al., 2013) and seawater.

5.2. *Distinguishing subduction-derived vs late-stage δ^{37}Cl signatures*

The SCLM beneath the southwestern United States was likely enriched in the heavy halogens (Segee-Wright et al., 2023) and fluid-mobile elements (Lee, 2005; Marshall et al., 2017b) from dehydration or melting of the subducted Farallon plate. Xenolith δ^{37}Cl values that are >1.5 ‰ above the mantle range further indicate a Cl source other than the depleted mantle. Subducted components are a likely Cl source; however, late-stage Cl additions from shallow crustal fluids may also contribute Cl that is not mantle-derived and must be filtered to determine the δ^{37}Cl value of the slab-derived component.

Xenoliths from the Navajo Volcanic Field contain two texturally distinct generations of hydrous minerals: early-stage hydrous minerals formed in the lithospheric mantle and late-stage serpentine that is likely syn- or post-emplacement (e.g. Smith, 1979, 2010). Early-stage hydrous minerals include antigorite, amphibole, chlorite, phlogopite, and clinohumite that formed in the mantle at temperatures of 530–650 °C (Smith, 2013). Hydrogen isotope values of the early-stage hydrous minerals range from −79 ‰ to −33 ‰ (Marshall et al., 2017b), which are consistent with formation from a subduction-derived fluid and inconsistent with formation from a meteoric fluid (Marshall et al., 2017b). Early-stage hydrous minerals are suggested to have formed from fluids ultimately derived from the Farallon plate (e.g. Smith, 2010; Marshall et al., 2017b). Chlorine is strongly hydrophilic and partitions much more strongly into the hydroxyl group of hydrous minerals than into nominally anhydrous mantle minerals (e.g. Frezzotti and Ferrando, 2018; Klemme and Stalder, 2018). This means most Cl will likely be hosted in hydrous minerals. Therefore, the δ^{37}Cl values of the early-stage hydrous minerals will also reflect the δ^{37}Cl composition of the Farallon-derived fluid. For samples with <30 % late-stage serpentine relative to early-

stage hydrous minerals, the bulk rock δD values (-84 ‰ to −48 ‰) are similar to the range of early-stage hydrous mineral separates from Marshall et al., (2017b). This suggests that the bulk δ^{37}Cl values of those samples with < 30 % of late-stage serpentine will likely reflect the composition of the Farallon-derived fluid.

However, because late-stage serpentine may contain significant quantities of Cl, it likely contributes to the δ^{37}Cl value of the bulk xenolith. Samples for which late-stage serpentine composes >90 % of hydrous minerals have bulk rock δD values of −122 ‰ to −101 ‰. Because the late-stage serpentine is the primary water-bearing phase in these samples and it is unlikely that structurally bound water in nominally anhydrous minerals will contribute significant quantities of water to the bulk sample (Navajo Volcanic Field xenolith pyroxene water content = 38–588 ppm; Marshall et al., 2018), these δD values of −122 to −101 ‰ are assumed to be representative of the late-stage serpentine. Assuming that the late-stage serpentine formed at 50 to 500 °C, lower than the equilibrium temperature of the early-stage hydrous minerals, the calculated equilibrium fluid δD values that formed the late-stage serpentine range from approximately −59 ‰ to −94 ‰, respectively (Saccocia et al., 2009). These values are similar to the range of modern groundwater at Green Knobs and Moses Rock (δD = −76 ‰ to −77 ‰; Bowen and Revenaugh, 2003; Bowen, 2022), consistent with formation from interaction with groundwater or shallow crustal fluids. Paleoelevation estimates suggest that the altitude of the Navajo Volcanic Field has not changed dramatically since 20–30 Ma when the SUM diatremes were emplaced (Heitmann et al., 2021). Therefore, modern meteoric water δD values are likely representative of those present during the emplacement of the xenolith-bearing SUM diatremes.

The positive correlation between bulk rock δD values and the calculated proportion of early-stage to total hydrous minerals (Fig. 6) indicates that the 74 ‰ range in bulk rock δD value is due to mixing of subduction-derived water with a high δD value and meteoric/ continental crustal water with a low δD value. Additionally, the positive correlation between bulk rock δD and δ^{37}Cl values (Fig. 4) indicates that subduction-derived fluids have high δ^{37}Cl values. Samples with the lowest bulk δD values (−122 ‰ to −101 ‰) and largest proportion of late-stage serpentine also have δ^{37}Cl values of + 0.1 ‰ to +0.8 ‰, whereas those with the highest bulk δD values (−84 ‰ to −51 ‰) and higher proportions of early-stage hydrous minerals have δ^{37}Cl values ≈ +1.0 ‰ to + 1.9 ‰. The range of δD and δ^{37}Cl values can be explained by mixing of early-stage hydrous minerals with δ^{37}Cl values ≈+1.0 ‰ to +2.0 ‰ and [Cl] = 100–2000 ppm with late-stage serpentine with δ^{37}Cl values ≈+0.0 ‰ to +0.3 ‰ and [Cl] ≈ 700–3000 ppm (Fig. 4; see supplementary material for details). The majority of the isotope values can be explained by mixing of late-stage hydrous minerals with early-stage hydrous minerals that either have variable isotope ratios within the endmember range (red curves in Fig. 4) or that have homogenous isotope compositions but heterogeneous Cl concentrations (black curves in Fig. 4).

Cl isotope ratios form only a weak trend with the calculated proportion of early-stage to total hydrous minerals (non-directional p-value = 0.1; Supplementary Figure S1). This could be due to multiple subducted Cl isotope compositions but may also simply be due to variable [Cl] of different hydrous minerals resulting in multiple mixing trends (see supplementary material). Therefore, we interpret that the Farallon-derived δ^{37}Cl signature in the North American SCLM is + 1.0 to + 1.9 ‰, whereas the late-stage serpentine δ^{37}Cl signature is likely < 0.3 ‰. The Cl isotope signature of the late-stage serpentine is consistent with North American continental crustal fluids from Texas, the Gulf of Mexico, the Canadian Shield, and the Michigan Basin with an average δ^{37}Cl value ≈ −0.2 ± 0.5 ‰ (Barnes and Sharp, 2017 and references therein), likely introduced during emplacement of the SUM diatremes.

5.3. Preservation of slab-derived δ^{37}Cl in Elephant Butte SCLM xenolith

Unlike the Navajo Volcanic Field xenoliths, the refractory Elephant Butte SCLM xenolith has only moderate Cl enrichment ([Cl] = 17 ppm; Cl/Nb = 26; Fig. 3) yet contains elevated δ^{37}Cl (+1.2 ‰; Fig. 3) similar to the Farallon-derived range in the Navajo Volcanic Field. Rowe et al. (2015) suggested that the SCLM beneath the southern Rio Grande Rift was enriched in Cl from a Farallon-derived fluid/melt. However, Cl enrichment was ephemeral, preserved only in older (>38 Ma) melt inclusions (Rowe et al., 2015). Lower, mantle-like Cl/Nb in younger southern Rio Grande Rift melt inclusions may not be due to a lack of hydration, but rather the loss of volatiles due to either devolatilization from progressive volcanism or thermal erosion of the metasomatized SCLM (Rowe et al., 2015). The SCLM xenoliths from Elephant Butte in this study are hosted in young (<5 Ma) basalts, and so Cl/Nb only slightly higher than the depleted mantle is consistent with melt inclusions data from the southern Rio Grande Rift (Rowe and Lassiter, 2009; Rowe et al., 2015). Based on the high δ^{37}Cl value, we suggest that the Farallon-derived δ^{37}Cl signature was preserved despite Cl loss.

5.4. Source of high δ^{37}Cl values in Navajo xenoliths

Bulk chlorine concentrations (31–320 ppm; Fig. 3a) and Cl/Nb (100–7000; Fig. 3b) of Navajo Volcanic Field xenoliths that have little or no late-stage serpentine are 3–100 times higher than in the depleted mantle range (<1–7 ppm) (Segee-Wright et al., 2023). Such extreme enrichment in Cl and Cl/Nb suggests that almost all Cl in these samples is from a slab-derived fluid. If the pre-metasomatized SCLM contributed 0.5–3 ppm Cl to the xenoliths (based on the lower range of measured Cl contents of nearby anhydrous SCLM xenoliths; Segee-Wright et al., 2023), then subduction-derived Cl would comprise 90–99.8 % of the Cl in these xenoliths. For the Navajo xenolith with the lowest Cl concentration (N23-GN, [Cl] = 31 ppm), we calculate that the fluid that would result in the measured δ^{37}Cl value of +1.9 ‰ would need to have a δ^{37}Cl value between +2.0 ‰ and +2.1 ‰, very similar to the observed δ^{37}Cl value of the xenolith. For all other xenoliths with larger quantities of subduction-derived Cl, the δ^{37}Cl composition of the fluid and xenolith would likely be even more similar. Therefore, the δ^{37}Cl values of the xenoliths are likely an approximate reflection of the δ^{37}Cl values of the slab-derived fluid with little Cl contribution from the pre-metasomatized SCLM.

Because little Cl isotope fractionation occurs during the breakdown of hydrous minerals in subducted plates (Schauble et al., 2003; Barnes et al., 2006; Liebscher et al., 2006; Bonifacie et al., 2008b; John et al., 2011; Selverstone and Sharp, 2015; Balan et al., 2019; Barnes et al., 2019), the δ^{37}Cl value of the released fluids will reflect the δ^{37}Cl value of the subducted component that dehydrated. The fluids released from the dehydration of the subducted plate then migrate upward into the overlying SCLM mantle and form hydrous minerals in the SCLM. Estimates of the temperature at which this hydration occurs are 400–650 °C (Smith, 2013). Any equilibrium Cl isotope fractionation between hydrous minerals and the fluid would also be small at these temperatures ($1000\ln\alpha_{(\text{hydrous mineral-fluid})} \leq +0.2$ ‰ to +0.5 ‰; Schauble et al., 2003; Balan et al., 2019). While this fractionation can explain a small portion of the δ^{37}Cl isotope range, it cannot account for values as high as +1.9 ‰ (Fig. 2). Therefore, the high δ^{37}Cl values of these xenoliths likely reflect ^{37}Cl enrichment of the dehydrating component in the subducted plate.

Although the SCLM beneath the Colorado Plateau has experienced Proterozoic subduction (e.g. Selverstone et al., 1999), previous studies indicate that the hydration of the SCLM beneath the Navajo Volcanic Field occurred since 30–80 Ma and is likely associated with the recent shallow-slab subduction of the Farallon plate (Smith, 1979, 2010; Smith et al., 2004). The similarity of the subduction-related δ^{37}Cl signature in xenoliths from Green Knobs (δ^{37}Cl = +1.0 ‰ to +1.9 ‰) and Moses Rock (δ^{37}Cl ≈ +1.6 ‰) across the Yavapai-Mazatzal suture (Fig. 1) supports Farallon-derived metasomatism over Proterozoic metasomatism. During Proterozoic subduction, the Mazatzal terrane subducted to the northwest under the Yavapai terrane (Selverstone et al., 1999). This northwest subduction resulted in hydration of the Yavapai

province SCLM, but not the Mazatzal. If Proterozoic subduction were the source of ^{37}Cl enrichment in these xenoliths, it would only be present to the northwest of the suture at Moses Rock and would be lacking at Green Knobs. Furthermore, a similar ^{37}Cl enrichment in the refractory Elephant Butte xenolith ($\delta^{37}Cl = +1.2$ ‰; calculated metasomatizing fluid has $\delta^{37}Cl$ values of +1.2 ‰ to +1.7 ‰) further supports a more widespread Farallon-derived source of Cl over more localized Proterozoic subduction.

Components of subducted oceanic plates have different ranges of $\delta^{37}Cl$ values (Fig. 2; Barnes and Sharp, 2017). While there are several subducted lithologies that overlap with the Farallon-derived $\delta^{37}Cl$ signature (+1.0 ‰ to +1.9 ‰), fewer of these lithologies would retain water and Cl to eclogite facies conditions and have oxygen isotope ratios that explain the low $\delta^{18}O$ values in the xenoliths (Fig. 5). Terrigenous sediments, for example, can have $\delta^{37}Cl$ values of up to +1.8 ‰ (Selverstone and Sharp, 2015), but a sediment-derived fluid or melt would

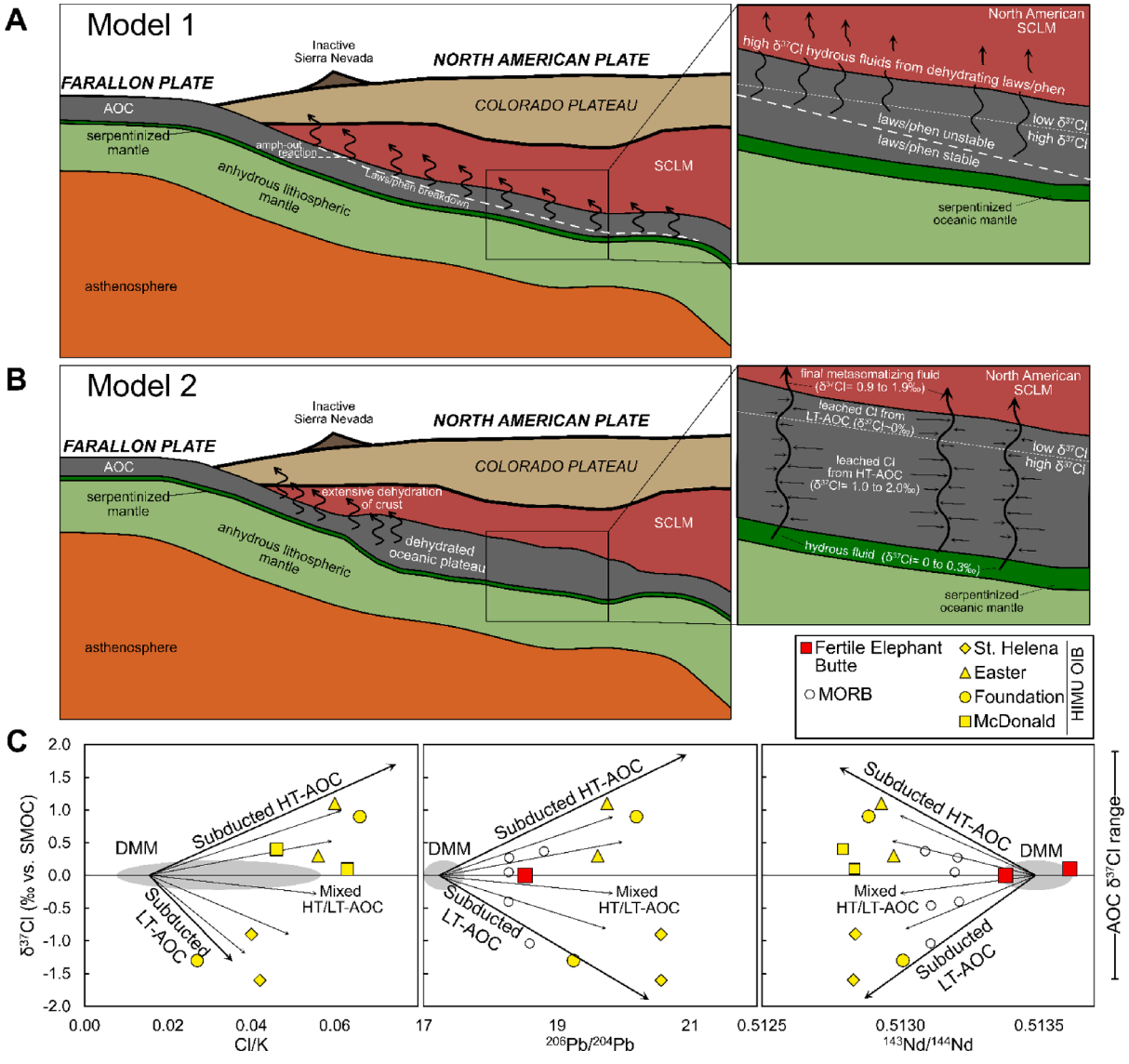

Fig. 7. (A) Schematic illustration of Model 1. Amphibole in the subducted Farallon crust dehydrates at ~90 km depth (dotted line). Lawsonite and phengite at the top of the subducting plate begin to break down due to conductive heating (dashed line). Lawsonite and phengite (laws/phen) in the lower crust remain stable until they are heated beyond their stability field (dashed line is the boundary between stable and unstable conditions). Beneath the Colorado Plateau, lawsonite/phengite (laws/phen) in the lower crust are unstable, releasing hydrous fluids with high $\delta^{37}Cl$ values relative to depleted mantle. This fluid then metasomatizes the overlying SCLM. (B) Schematic illustration of Model 2. The entire Farallon crust is largely dehydrated before reaching depths beneath the Colorado Plateau (120–130 km). Serpentinized Farallon oceanic mantle remains stable due to its location in the cold core of the subducted plate. Subducted serpentinite dehydrates beneath the Colorado Plateau, releasing hydrous fluids that travel through the overlying subducted oceanic plateau. Residual Cl in the dehydrated oceanic plateau is leached by the serpentinite-derived fluids, imparting a crustal $\delta^{37}Cl$ signature. Because the crust is so thick, HT-AOC composes a larger portion of the crust than LT-AOC, resulting in a net increase in $\delta^{37}Cl$ value in the final fluid that interacts with the overlying SCLM. (C) $\delta^{37}Cl$ values plotted against Cl/K, $^{206}Pb/^{204}Pb$, and $^{143}Nd/^{144}Nd$ for HIMU OIB glasses (John et al., 2010), MORB glasses (Sharp et al., 2007), and mantle xenoliths (this study). MORB [K] and radiogenic isotope data from PetDB database (www.earthchem.org/petdb; see supplementary material for individual references). HIMU glasses with $\delta^{37}Cl$ values higher than DMM have slightly higher Cl/K than ones with lower $\delta^{37}Cl$ values, consistent with Model 1 (see Section 5.5.1 of text). HIMU glasses span almost the range of $\delta^{37}Cl$ values observed in AOC. Xenolith, MORB, and HIMU samples display more variation in $\delta^{37}Cl$ values at more radiogenic Pb and Nd, consistent with addition of subducted AOC in the HIMU mantle. (HT-), (LT)-AOC=(high-temperature), (low-temperature)-altered oceanic crust; SCLM = sub-continental lithospheric mantle; amph = amphibole; MORB = mid-ocean ridge basalt; DMM = depleted MORB-source mantle. DMM Cl/K ratios are based on estimates from Saal et al. (2002) and Kendrick et al. (2017).

have $\delta^{18}O$ values higher than average mantle values (Eiler, 2001). Marshall et al., (2017b) proposed high-temperature altered oceanic crust (HT-AOC) and/or serpentinized mantle in the subducted Farallon plate as the sources of the metasomatic fluid in the SCLM beneath the Navajo Volcanic Field based on elevated hydrous mineral δD values and low $\delta^{18}O_{olv}$ relative to the average mantle. These are the two subducted lithologies likely dehydrated last due to their distance from the slab surface, and dehydration of both these lithologies can produce a fluid that would impart the observed δD (e.g., Shaw et al., 2018) and $\delta^{18}O$ (e.g., Gregory and Taylor, 1981; Eiler, 2001) compositions of the SCLM, and so cannot easily be distinguished as the fluid source. However, Cl isotope compositions of these reservoirs have different ranges (Fig. 2), and so can help distinguish between these sources. We explore these possible subducted fluid sources.

5.4.1. Model 1: Dehydration of subducted altered oceanic crust

High-temperature altered oceanic crust (HT-AOC) $\delta^{37}Cl$ values range from −0.6 ‰ to +1.8 ‰ (Fig. 2) with an average of +0.6 ‰ (Barnes and Cisneros, 2012). This range of values significantly overlaps the slab-derived $\delta^{37}Cl$ signature (+1.0 ‰ to +1.9 ‰) in the Elephant Butte and Navajo Volcanic Field SCLM xenoliths. Therefore, metasomatism of the North American SCLM from dehydration of altered oceanic crust could explain the observed $\delta^{37}Cl$ values. The $\delta^{18}O$ values of HT-AOC (0 to +6 ‰; Gregory and Taylor, 1981; Eiler, 2001) are lower than average mantle (+5.5 ‰; Eiler, 2001), consistent with the observed negative correlation between $\delta^{37}Cl$ and $\delta^{18}O_{cpx}$ values in these xenoliths (Fig. 5b).

However, the depth of the Farallon slab beneath the Colorado Plateau is estimated to be >120–130 km during shallow-slab subduction (Fig. 7a; Roden et al., 1990; Lee et al., 2001; West et al., 2004; Smith, 2013). Pressures at this depth are outside the amphibole stability field (Schmidt and Poli, 1998a, 1998b), so any amphibole in the crust is likely to have dehydrated. Because amphibole is the main host of Cl in HT-AOC (Barnes and Cisneros, 2012; Debret et al., 2016; Kendrick et al., 2019a, 2019b) and Cl is expected to largely partition into the fluid phase, most Cl from the altered oceanic crust may have been lost before reaching the Colorado Plateau.

However, it is plausible that other high pressure hydrous minerals such as lawsonite or phengite in eclogitized metagabbros could retain Cl and high $\delta^{37}Cl$ values after loss of amphibole to depths of up to >200 km (Schmidt and Poli, 1998a). Lawsonite and phengite contain ~11.5 wt% and ~ 4 wt% H_2O, respectively, and both can contain similar Cl contents as coexisting amphibole (Debret et al., 2016; Pagé et al., 2016). Therefore, lawsonite-and phengite-eclogites may retain significant water and Cl after the dehydration of amphibole in the subducted crust. Lawsonite- and phengite-bearing eclogites are present beneath the Colorado Plateau (e.g. Usui et al., 2003), indicating that lawsonite and phengite were stable at P-T conditions of the Farallon plate beneath the Colorado Plateau and so could retain water and Cl in the Farallon crust to depths below the Colorado Plateau (Fig. 7a).

While lawsonite and phengite do not occur in large abundance in most exhumed eclogites, this paucity may be the result of retrograde reactions, not low abundance in subducted crust (Whitney et al., 2020 and references therein). Hacker (2008) and van Keken et al. (2011) suggest that metagabbroic phengite- and lawsonite-eclogites dominate the post-arc water budget of global subducted crust, whereas metabasaltic upper crust is largely dehydrated beneath the arc front. Preferential retention of lawsonite and phengite in Farallon metagabbroic eclogites over metabasaltic eclogite to depths below the Colorado Plateau can account for the HT-AOC-like $\delta^{37}Cl$ values (Fig. 2), the high water contents, δD values greater than typical mantle values, and lower $\delta^{18}O_{cpx}$ values of SCLM xenoliths in the Navajo Volcanic Field. SUM-hosted lawsonite- and phengite-bearing eclogite xenoliths have been found on the Colorado Plateau and have been interpreted as crustal fragments of the subducted Farallon plate (Helmstaedt and Doig, 1975; Usui et al., 2003). However, several subsequent studies argue that these eclogite xenoliths are subducted Proterozoic crust that has been hydrated by Farallon-related fluids (Smith et al., 2004; Smith and Griffin, 2005). Regardless of their origin, the presence of these lawsonite- and phengite-bearing eclogites beneath the Colorado Plateau indicates the stability of those minerals at depth. Therefore, a plausible source of metasomatizing fluids that hydrated the Colorado Plateau SCLM is the breakdown of phengite and lawsonite in HT-AOC in the subducted Farallon plate.

5.4.2. Model 2: Leaching of residual Cl in dehydrated altered oceanic crust

Several previous studies have suggested serpentinized oceanic mantle in the cold core of the subducted Farallon plate as the source of metasomatic enrichment of the SCLM underlying the Colorado Plateau and the SW United States in general (Lee, 2005; Li et al., 2008; Marshall et al., 2017b). Serpentinized oceanic mantle in the Farallon plate would likely be the last part of the slab to dehydrate (English et al., 2003), and so could have retained its volatile content to depths beneath the Colorado Plateau and Rio Grande Rift. However, most seafloor serpentinites have $\delta^{37}Cl$ values of −1.6 ‰ to +0.5 ‰ (Fig. 2; Barnes and Sharp, 2017 and references therein), falling well below the range in these SCLM xenoliths. Some obducted serpentinites have $\delta^{37}Cl$ values that range up to + 2.4 ‰, but these values may be the result of infiltration of a sediment-derived external fluid during obduction, and so are not representative of average subducted serpentinite (Selverstone and Sharp, 2015; Barnes et al., 2014a). Higher than average $\delta^{37}Cl$ values in serpentinites could result from preferential retention of structurally bound Cl (Fig. 2) and the removal of water-soluble Cl. Chlorine isotope ratios of structurally bound Cl are on average ~0.2 ‰ higher than the water-soluble Cl fraction in serpentinites and can reach values of +1.0 ‰ to +1.8 ‰ (Fig. 2) (Barnes and Sharp, 2006; Barnes et al., 2009b). However, less than three percent of serpentinites measured have structurally bound Cl with $\delta^{37}Cl$ values > +1.0 ‰ (Fig. 2), and so preferential subduction of structurally bound Cl in serpentinite is unlikely to be the source of elevated $\delta^{37}Cl$ values in the xenoliths. Therefore, it is unlikely that dehydration of serpentinized mantle in the Farallon plate is the sole source of Cl enrichment in the North American SCLM.

While serpentinite dehydration alone cannot account for the observed high $\delta^{37}Cl$ values in the xenoliths of this study, previous studies have suggested that serpentinite-derived fluids interact with the overlying eclogitized Farallon crust and either induce melting in devolatilized eclogite (Lee, 2005) or leach trace elements from the eclogite (Marshall et al., 2017b). It is possible to obtain the observed high $\delta^{37}Cl$ values (+0.9 ‰ to +1.9 ‰) in the Navajo Volcanic Field xenoliths through dehydration of serpentine in subducted oceanic mantle and subsequent interaction with the overlying Farallon crust without the need for residual high-pressure hydrous minerals subducted to depths >120 km. The high $\delta^{37}Cl$ values can be obtained by leaching Cl from dehydrated eclogite in the subducted Farallon plate by a serpentinite-derived fluid. Hydrous fluids released during subcrustal serpentinite breakdown in the hydrated oceanic mantle of the subducted Farallon plate may have leached Cl from overlying parts of the subducted plate that had high $\delta^{37}Cl$ values (Fig. 7b). This leaching has been previously proposed to explain the fluid-mobile trace element enrichments in Navajo Volcanic Field xenoliths (Marshall et al., 2017b). HT-AOC can have $\delta^{37}Cl$ values up to +1.8 ± 0.2 ‰ (Fig. 2; Barnes and Cisneros, 2012), and so could account for the elevated $\delta^{37}Cl$ values in these xenoliths.

However, leaching of Cl from subducted eclogite can only impart an elevated Cl isotope signature on a serpentine-derived fluid if the residual dehydrated eclogite has high [Cl] (65–200 ppm) and the lower crust preferentially contributes Cl to the serpentinite-derived fluid, or if the eclogitized oceanic crust is overthickened. This is due to mass balance constraints required by the relatively low Cl content of eclogite (5–200 ppm Cl; Philippot et al., 1998; Debret et al., 2016; Pagé et al., 2016; Hughes et al., 2018; Urann et al., 2020; Beaudoin et al., 2022) compared to the Cl content of final fluids derived from the late dehydration of deeply subducted serpentinite (Kendrick et al., 2011). For leached

altered oceanic crust to impart a $\delta^{37}Cl$ signature on the serpentinite-derived fluid, the leached crust must contribute a significant quantity of Cl to the fluid relative to the serpentinite fluid source. If the Farallon plate had a "Penrose-style" structure with 2 km of dehydrated gabbroic eclogite, then the dehydrated HT-AOC would need to contain at least 65 ppm Cl for $\delta^{37}Cl$ values of the fluid to reach the moderate slab-derived signature (+1.5 ‰) present in the Navajo Volcanic Field xenoliths and would need at least 200 ppm Cl to reach $\delta^{37}Cl$ values of +1.8 ‰. These calculations assume 100 % of the Cl in the overlying crust is leached (see supplementary material for calculation details), which is unlikely given frequently observed channelized flow in eclogites (e.g. Spandler and Hermann, 2006; Spandler et al., 2011). If the leaching efficiency were only 50 %, then the HT-AOC would require at least 400 ppm Cl to impart a $\delta^{37}Cl$ values of +1.8 ‰.

This range of crustal Cl contents is higher than concentrations measured in most obducted and alpine eclogites (7–23 ppm Cl; Hughes et al., 2018; Urann et al., 2020; Beaudoin et al., 2022). Additionally, this requires the preferential retention of Cl in the dehydrated gabbroic eclogite relative to basaltic eclogite (average basaltic altered oceanic crust $\delta^{37}Cl$ value ≈ 0 ‰; Barnes and Cisneros, 2012). There is no *a priori* reason for this to be true in an *anhydrous* eclogite (presence of high-pressure hydrous minerals proposed in Model 1 is an *a priori* reason). Therefore, it is unlikely that leaching of a dehydrated "Penrose-style" Farallon plate would produce the observed elevated xenolith $\delta^{37}Cl$ values.

However, the Farallon plate undergoing flat-slab subduction during the Laramide orogeny may not have had a Penrose-style structure. Numerical modelling (English et al., 2003; Liu and Currie, 2016) and geophysical evidence (Liu et al., 2008) indicate that the flat-slab subduction was due, in part, to subduction of an 18 km thick oceanic plateau (Liu and Currie, 2016) that was the conjugate of the Hess or Shatsky Rise (Livaccari et al., 1981). Additionally, the Farallon plate may have been further hydrated by extensive slab-bend faulting. The Farallon plate was old (>50–100 Myr; Engebretson et al., 1984) when it subducted beneath the North American plate, and so may have been cold enough to fully hydrate the crust. While an increase in the Farallon plate thickness may have reduced the degree of slab-bend faulting, such faulting and extensive hydration is observed in the subducting Hikurangi Plateau (e.g. Herath et al., 2020) with a crust thickness of ~12 km. After accounting for full hydration of an 18 km thick oceanic Farallon crust, and assuming hydration below ~2000 mbsf is dominated by amphibole with high $\delta^{37}Cl$ values (Barnes and Cisneros, 2012), leaching of dehydrated eclogitized altered oceanic crust with only ~10–25 ppm Cl can result in the high $\delta^{37}Cl$ signature observed in the Navajo volcanic Field xenoliths (see supplementary information for calculation details). These concentration ranges overlap those measured in eclogite xenoliths and obducted eclogites (5–23 ppm; Hughes et al., 2018; Urann et al., 2020; Beaudoin et al., 2022).

Therefore, it is possible that the observed high $\delta^{37}Cl$ values in the SCLM xenoliths are from a serpentinite-derived fluid that leached significant amounts of Cl from an overlying thick crust of a subducted oceanic plateau in the Farallon plate. However, this model requires perfectly efficient leaching of a thick subducted crust in addition to the correct balance of Cl concentrations in the subducted crust and serpentinite. The complex multistep processes and narrow range of parameters that allow this model to explain the observed isotope compositions of the xenoliths lead us to believe that Model 2 is less likely than Model 1.

5.5. Predictions and Implications of the Different Models

Model 1 and Model 2 can potentially both explain the observed high $\delta^{37}Cl$ values, high bulk water contents, and low $\delta^{18}O_{cpx}$ values, and high early-stage hydrous mineral δD values of SCLM xenoliths in the Navajo Volcanic Field. The two models are not mutually exclusive, and a thick, hydrated oceanic plateau may help to explain the preservation of lawsonite in the lower crust to great depths. However, the main difference between the two models is the presence (Model 1) or absence (Model 2) of high-pressure hydrous minerals and residual Cl in deeply subducted oceanic crust. This difference has implications on the quantity and isotopic composition of oceanic crustal Cl globally subducted past the arc front.

5.5.1. Model 1 Predictions and Implications

Model 1 requires residual Cl in lawsonite/phengite in deeply subducted lower crustal eclogite, whereas upper crustal eclogites are largely depleted in Cl, consistent with models of Hacker, (2008) and van Keken et al., (2011) for intermediate to cold subduction zones. The preferential retention of Cl in the lower crust relative to the upper crust would result in higher average $\delta^{37}Cl$ value of the deeply subducted crust than the average altered oceanic crustal $\delta^{37}Cl$ value on the seafloor, skewing the recycled crustal $\delta^{37}Cl$ values in the mantle towards more positive values. Continuous preferential subduction of lower crustal Cl would result in an increase in the average mantle $\delta^{37}Cl$ value over time. Quantification of the secular shift in the average convecting mantle $\delta^{37}Cl$ value over time depends on volatile recycling efficiency, the extent of lithosphere hydration, the Cl content of lawsonite and phengite, and the age of modern-style subduction. Concurrent subduction of serpentine in hydrated oceanic mantle lithosphere (average $\delta^{37}Cl$ ≈+0.2 to +0.3 ‰; Barnes and Sharp, 2017) would also increase the average $\delta^{37}Cl$ value of the convecting mantle. Based on endmember conditions (see supplementary material), we calculate that the $\delta^{37}Cl$ value of the bulk convecting mantle would increase by a maximum of 0.5 ‰ over 3 Ga of modern-style subduction. The dependence of this quantification on a wide range of poorly known parameters makes this calculation highly qualitative and likely overestimates the shift in the bulk convecting mantle $\delta^{37}Cl$ value. However, this calculation demonstrates that the $\delta^{37}Cl$ value of the bulk mantle will not change significantly even when considering high fluxes of Cl into the convecting mantle.

While the bulk $\delta^{37}Cl$ value of the convecting mantle is unlikely to significantly change, melts that sample high concentrations of subducted crustal volatiles in the mantle, such as HIMU basalts (e.g. Hofmann, 1997) or metasomatized SCLM, may dramatically change. Model 1 requires higher Cl concentrations in the lower subducted crust subducted, whereas the upper crust is largely devolatilized. While this is unlikely to be applicable to all subduction zones due to variability in many thermal, kinematic, and geometric parameters (e.g. Syracuse et al., 2010), thermal modeling suggests it is likely applicable to cold subducting plates (van Keken et al., 2011; Shirey et al., 2021). Preservation of large contrasts in Cl concentration in subducted crust into the convecting mantle would result in large variations in Cl/Nb and Cl/K in HIMU (derived from partially dehydrated subducted oceanic crust; Hofmann and White, 1982). Such heterogenous distribution of Cl in subducted crust could explain contrasting conclusions drawn on the degree of Cl recycling in subducted altered oceanic crust sampled by HIMU basalts (~0% to 15–30 %; Lassiter et al., 2002; Hanyu et al., 2019). Additionally, relatively higher water contents would be coupled with higher Cl contents of deeply subducted high-temperature altered oceanic crust, resulting in variable [H_2O] and H_2O/Ce of HIMU basalts. Incorporation of subducted oceanic crust with variable water contents is consistent with observations of variable H_2O/Ce in HIMU (e.g., Jackson et al., 2015). Variable retention of volatiles in subducted crust complicates secular mass-balance calculation of volatile subduction (e.g., Bekaert et al., 2021) and must be considered in these calculations.

Variable incorporation of subducted upper vs lower crust in HIMU basalts will result in HIMU basalts spanning the full range of altered oceanic crust $\delta^{37}Cl$ values (−1.6 ‰ to + 1.8 ‰; Fig. 7c; Barnes and Cisneros, 2012). However, because lower crustal eclogites would retain greater quantities of Cl and H_2O into the convecting mantle, HIMU basalts with elevated $\delta^{37}Cl$ values should extend to higher Cl/K, Cl/Nb, and H_2O/Ce. This prediction generally agrees with Cl/K and $\delta^{37}Cl$ data from the only study of Cl isotopes in HIMU glasses (Fig. 7c; John et al.,

2010), though the offset is not large, and interpretations are complicated by the small dataset (n = 6) and loss of K from the subducting plate during prograde metamorphism (e.g., Becker et al., 2000). Currently, there is not sufficient data to determine whether such trends also exist for Cl/Nb or H_2O/Ce. Further work must be conducted on coupled Cl/Nb, H_2O/Ce, and δ^{37}Cl values of HIMU basalts to test this model.

Additionally, diamonds from the North American SCLM host saline high-density fluid inclusions with compositions suggesting an oceanic crust origin of the fluid (Weiss et al., 2015). Preservation of high-pressure hydrous minerals that carry volatile elements into the deep interior of cratons can explain the presence of these crustally-derived saline fluids. The Cl isotope evidence presented here provides a second, independent line of evidence supporting subducted oceanic crustal Cl in the North American SCLM. Future work examining the Cl isotope composition of lithospheric or transition zone diamond fluid inclusions could elucidate additional sources of volatiles in the SCLM or transition zone. Currently, only one diamond has been analyzed for its Cl isotope composition (δ^{37}Cl value = −0.15 ‰; Sharp et al., 2013). This remains an area ripe for future research.

5.5.2. Model 2 Predictions and Implications

Model 2 suggests that the subducted Farallon crust is largely dehydrated and retains little Cl or H_2O, and so the only reason for the observed crustal signature is leaching of a thick oceanic plateau. This model requires that dehydration of serpentinized mantle beneath an oceanic plateau will efficiently leach Cl and other fluid-mobile elements out of the overlying plate, largely overprinting the δ^{37}Cl of the serpentinite-derived fluid. This leaching could result in large variation in the δ^{37}Cl values of SCLM far from trenches above other subducted oceanic plateaus. While Model 2 predicts that δ^{37}Cl values of metasomatized SCLM above subducted oceanic plateaus will be generally positive, the actual δ^{37}Cl value would largely depend on degree of serpentinization of the subducted oceanic mantle and channelization of fluid flow.

Model 2 predicts that both subducted upper and lower crust are largely dehydrated by the time they reach eclogite facies conditions. This implies that the HIMU mantle source has low [Cl] and [H_2O] and that the HIMU basalts that incorporate subducted oceanic crust will have low Cl/K and Cl/Nb regardless of their incorporation of subducted upper or lower oceanic crust. Therefore, there should be no systematic difference in Cl/K, Cl/Nb, or H_2O/Ce for HIMU samples with high δ^{37}Cl vs low δ^{37}Cl values (high-temperature altered crust vs low-temperature crust). This is not consistent with the data of John et al. (2010), though current δ^{37}Cl data on HIMU basalts are limited. Additionally, efficient loss of Cl from eclogitized crust would result in little to no Cl, Cl/K, or Cl/Nb enrichment in all HIMU basalts, consistent with the conclusions of Lassiter et al. (2002), but inconsistent with elevated Cl/K and Cl/Nb values in HIMU basalts (Stroncik and Haase, 2004; Hanyu et al., 2019) and high calculated [Cl] in the HIMU mantle source (~20–37 ppm Cl; Cabral et al., 2014; Le Voyer et al., 2015).

Overall, the predictions made by Model 2 for δ^{37}Cl values, Cl/K, and Cl/Nb of HIMU basalts do not match the current dataset as well as the predictions made by Model 1. Additionally, the mechanism of Model 1 is simpler and less dependent on various model parameters. Therefore, we prefer Model 1. However, this work is nascent, and additional δ^{37}Cl data must be collected in both metasomatized SCLM and HIMU basalts to further test the model. Regardless of the correct model, the observed high δ^{37}Cl values indicate that subducted oceanic crust can introduce significant Cl isotope heterogeneity beyond the arc front. While subduction of these high δ^{37}Cl values into the convecting mantle is unlikely to dramatically change the overall δ^{37}Cl value of the convecting mantle, it can cause large local Cl isotope heterogeneity in the mantle. Such heterogeneity may be sampled by MORB, OIB, mantle xenoliths, and intracontinental melts.

6. Conclusions

Fertile peridotite xenoliths from Elephant Butte have δ^{37}Cl values of 0.0 ‰ to +0.1 ‰, consistent with seawater/chondrite-like δ^{37}Cl values in the convecting mantle. In contrast, high δ^{37}Cl values (+0.9 ‰ to +1.9 ‰) of the Navajo and refractory Elephant Butte SCLM xenoliths deviate significantly from this average mantle value, suggesting the addition of Cl derived from subducted high-temperature-altered oceanic crust in the Farallon plate over a broad region of the North American SCLM. Cl isotope values ≈+0.1 to +0.8 ‰ in xenoliths with significant syn/post-emplacement serpentinization are due to a second contribution of Cl from late-stage crustally-derived fluids with δ^{37}Cl values < 0.3 ‰.

The subducted lower crustal, high δ^{37}Cl signature was likely carried into the North American SCLM by a fluid produced by the breakdown of high-pressure hydrous minerals lawsonite or phengite in the subducted Farallon plate. However, it is also possible that dehydration of serpentinized mantle in the subducted Farallon plate entrained residual Cl from an overlying thick oceanic plateau on the subducted Farallon plate, resulting in a ^{37}Cl-enriched metasomatizing fluid. HT-AOC-like δ^{37}Cl values in SCLM beneath the Colorado Plateau demonstrates that crustal Cl can be retained in subducting plates to depths >120 km and distances ~700–1000 km from the trench. This retention could result in large Cl isotope heterogeneities in the convecting mantle, though it is unlikely to significantly alter the average δ^{37}Cl value of the bulk depleted mantle. Incorporation of subducted AOC in HIMU basalts will result in a heterogeneous δ^{37}Cl value of the HIMU mantle. Both the SCLM and convecting mantle are likely heterogeneous in Cl isotope ratios due to subduction. Further work exploring the distribution of Cl isotope heterogeneities in the lithosphere and asthenosphere will allow for better constraints on Cl recycling into the mantle.

Data availability

Data are available through Mendeley Data at https://doi.org/10.17632/jvchrp92f2.1.

Declaration of competing interest

The authors declare that they have no known competing financial interests or personal relationships that could have appeared to influence the work reported in this paper.

Acknowledgements

This work is supported by funding by NSF-EAR-1850749 to J.D.B. and J.C.L. We would like to thank E. Marshall for his work collecting a subset of the oxygen isotope data, M. Riley for assistance preparing samples for hydrogen isotope analyses, J. Cullen for assistance collecting hydrogen and chlorine isotope data at UT Austin, and D. Smith for feedback on early drafts of the manuscript. This work uses samples that were previously collected on Navajo Lands, with permission from the Navajo Nation. This manuscript benefitted from constructive comments by three anonymous reviewers and editor Rosemary Hickey-Vargas.

Appendix A. Supplementary material

The Supplementary Material includes: (Section 1) hydrous mineral modal abundances (Table S1), as well as equations and assumptions associated with the modal abundance calculations; (Section 2) assumptions and equations used to calculate the fluid composition associated with sample N23-GN; (Section 3) endmember compositions (Table S2) and explanations for the mixing models in Fig. 4; (Section 4) component compositions (Table S3) and calculations used to determine the final Cl isotope ratio of serpentine-derived fluids in Model 2 after leaching of Cl from the overlying metabasalt and metagabbro, (Section 5) assumptions and calculations used to determine the maximum extent

of secular change to the average mantle Cl isotope ratio; and (Section 6) previously published Cl concentrations, trace element concentrations, and radiogenic isotope ratios of the SCLM xenolith in this study (Table S4) that are referred to in the figures and text. Supplementary material to this article can be found online at https://doi.org/10.1016/j.gca.2023.11.030.

References

Anderson, J.L., Morrison, J., 2005. Ilmenite, magnetite, and peraluminous Mesoproterozoic anorogenic granites of Laurentia and Baltica. Lithos 80, 45–60.

Balan, E., Créon, L., Sanloup, C., Aléon, J., Blanchard, M., Paulatto, L., Bureau, H., 2019. First-principles modeling of chlorine isotope fractionation between chloride bearing molecules and minerals. Chem. Geol. 525, 424–434.

Baldridge, W.S., Damon, P.E., Shafiqullah, M., Bridwell, R.J., 1980. Evolution of the central Rio Grande rift, New Mexico: New potassium-argon ages. Earth Planet. Sci. Lett. 51 (2), 309–321.

Barnes, J.D., Cisneros, M., 2012. Mineralogical control on the chlorine isotope composition of altered oceanic crust. Chem. Geol. 326–327, 51–60.

Barnes, J.D., Sharp, Z.D., Fischer, T.P., 2008. Chlorine isotope variations across the Izu-Bonin-Mariana arc. Geol 36, 883–886.

Barnes, J.D., Sharp, Z.D., Fischer, T.P., Hilton, D., Carr, M.J., 2009a. Chlorine isotope variations along the Central American volcanic front and back arc. Geochem Geophys Geosyst. 10, Q11S17.

Barnes, J.D., Paulick, H., Sharp, Z.D., Bach, W., Beaudoin, G., 2009b. Stable isotope ($\delta^{18}O$, δD, $\delta^{37}Cl$) evidence for multiple fluid histories in mid-Atlantic abyssal peridotites (ODP Leg 209). Lithos 110, 83–94.

Barnes, J.D., Beltrando, M., Lee, C.-T.A., Cisneros, M., Loewy, S., Chin, E., 2014a. Geochemistry of Alpine serpentinites from rifting to subduction: a view across paleogeographic domains and metamorphic grade. Chem. Geol. 389, 29–47.

Barnes, J.D., Straub, S.M., 2010. Chlroine stable isotope variaitons in Izu Bonin tephra: implications for serpentinite subduction. Chem. Geol. 272, 62–74.

Barnes, J.D., Penniston-Dorland, S.C., Bebout, G.E., Hoover, W., Beaudoin, G.M., Agard, P., 2019. Chlorine and lithium behavior in metasedimentary rocks during prograde metamorphism: A comparative study of exhumed subduction complexes (Catalina Schist and Schistes Lustrés). Lithos 336–337, 40–53.

Barnes, J.D., Prather, T., Cisneros, M., Befus, K., Gardner, J.E., Larson, T.E., 2014b. Stable chlorine isotope behavior during volcanic degassing of H_2O and CO_2 at Mono Craters, CA. Bull. Volcanol. 76, 805.

Barnes, J.D., Sharp, Z.D., 2006. A chlorine isotope study of DSDP/ODP serpentinized ultramafic rocks: insights into the serpentinization process. Chem. Geol. 228, 246–265.

Barnes, J.D., Selverstone, J., Sharp, Z.D., 2006. Chlorine chemistry of serpentinites from Elba, Italy, as an indicator of fluid source and subsequent tectonic history. Geochem. Geophys. Geosyst. 7, Q08015.

Barnes, J.D., Sharp, Z.D., 2017. Chlorine Isotope Geochemistry. Rev. Mineral. Geochem. 82, 345–378.

Beaudoin, G.M., Barnes, J.D., John, T., Hoffmann, J.E., Chatterjee, R., Stockli, D.F., 2022. Global halogen flux of subducting oceanic crust. Earth Planet. Sci. Lett. 594, 117750.

Becker, H., Jochum, K.P., Carlson, R.W., 2000. Trace element fractionation during dehydration of eclogites from high pressure terranes and the implications for element fluxes in subduction zones. Chem. Geol. 163, 6–99.

Behr, W.M., Smith, D., 2016. Deformation in the mantle wedge associated with Laramide flat-slab subduction. Geochem. Geophys. Geosyst. 17 (7), 2643–2660.

Bekaert, D.V., Turner, S.J., Broadley, M.W., Barnes, J.D., Halldórsson, S.A., Labidi, J., Wade, J., Walkowski, K.J., Barry, P.H., 2021. Subduction-Driven Volatile Recycling: A Global Mass Balance. Annu. Rev. Earth Planet. Sci. 49, 37–70.

Bennett, V.C., DePaolo, D.J., 1987. Proterozoic crustal history of the western United States as determined by neodymium isotopic mapping. GSA Bulletin 99, 674–685.

Bonifacie, M., Monnin, C., Jendrzejewski, N., Agrinier, P., Javoy, M., 2007. Chlorine stable isotopic composition of basement fluids of the eastern flank of the Juan de Fuca Ridge (ODP Leg 168). Earth Planet. Sci. Lett. 260, 10–22.

Bonifacie, M., Jendrzejewski, N., Agrinier, P., Humler, E., Coleman, M., Javoy, M., 2008a. The chlorine isotope composition of Earth's mantle. Science 319, 1518–1520.

Bonifacie, M., Busigny, V., Mével, C., Philippot, P., Agrinier, P., Jendrzejewski, N., Scambelluri, M., Javoy, M., 2008b. Chlorine isotopic composition in seafloor serpentinites and high-pressure metaperidotites: Insights into oceanic serpentinization and subduction processes. Geochim. Cosmochim. Acta 72, 126–139.

Bouvier, A.-S., Manzini, M., Rose-Koga, E.F., Nichols, A.R.L., Bamgartner, L.P., 2019. Tracing of Cl input into the sub-arc mantle through the combined analysis of B, O and Cl isotopes in melt inclusions. Earth Planet Sci Lett. 507, 30–39.

Bouvier, A.-S., Portnyagin, M.V., Flemtakis, S., Hoernle, K., Klemme, S., Berndt, J., Mironov, N.L., John, T., 2022a. Chlorine isotope behavior in subduction zone settings revealed by olivine-hosted melt inclusions from the Central America Volcanic Arc. Earth Planet Sci. Lett. 581, 117414.

Bouvier, A.-S., Rose-Koga, E.F., Chapuis, A., 2022b. Deciphering degassing and source effects in Cl isotopes in melt inclusions: the possible role of amphibole in the magma source of Stromboli (Aeolian Island Arc). Front. Earth Sci. 9, 793259.

Bowen, G.J., Revenaugh, J., 2003. Interpolating the isotopic composition of modern meteoric precipitation. Water Resources Res. 39 (10), 1299.

Bowen, G.J., 2022. The Online Isotopes in Precipitation Calculator, version 3.1. http://www.waterisotopes.org.

Broadley, M.W., Ballentine, C.J., Chavrit, D., Dallai, L., Burgess, R., 2016. Sedimentary halogens and noble gases within Western Antarctic xenoliths: implications of extensive volatile recycling to the sub continental lithospheric mantle. Geochim. Cosmochim. Acta 176, 139–156.

Byerly, B.L., Lassiter, J.C., 2012. Evidence from mantle xenoliths for lithosphere removal beneath the Central Rio Grande Rift. Earth Planet. Sci. Lett. 355–356, 82–93.

Cabral, R.A., Jackson, M.G., Koga, K.T., Rose-Koga, E.F., Hauri, E.H., Whitehouse, M.J., Price, A.A., Day, J.M.D., Shimizu, N., Kelley, K.A., 2014. Volatile cycling of H_2O, CO_2, F, and Cl in the HIMU mantle: a new window provided by melt inclusions from oceanic hotspot lavas at Mangaia, Cook Islands. Geochem. Geophys. Geosyst. 15, 4445–4467.

Chapin, C.E., 1979. Evolution of the Rio Grande Rift - a Summary. In: Riecker, R.E. (Ed.), Rio Grande Rift: Tectonics and Magmatism. American Geophysical Union, Washington D.C., pp. 1–5

Chiaradia, M., Barnes, J.D., Cadet-Voisin, S., 2014. Chlorine isotope variations across theQuaternary volcanic arc of Ecuador. Earth Planet. Sci. Lett. 396, 22–33.

Debret, B., Koga, K.T., Cattani, F., Nicollet, C., Van den Bleeken, G., Scwartz, S., 2016. Volatile (Li, B, F, and Cl) mobility during amphibole breakdown in subduction zones. Lithos 244, 165–181.

Eggenkamp, H.G.M., 1994. The geochemistry of chlorine isotopes. Ph.D. Thesis, Universiteit Utrecht, 151.

Eiler, J.M., 2001. Oxygen isotope variations of basaltic lavas and upper mantle rocks. Rev. Mineral. Petrol. 43 (1), 319–364.

Engebretson, D.C., Cox, A., Thompson, G.A., 1984. Correlation of plate motions with continental tectonics: Laramide to Basin-range. Tectonics 3 (2), 115–119.

English, J.M., Johnston, S.T., Wang, K., 2003. Thermal modelling of the Laramide orogeny: testing the flat-slab subduction hypothesis. Earth Planet. Sci. Lett. 214, 619–632.

Fischer, T.P., Ramírez, C., Mora-Amador, R.A., Hilton, D.R., Barnes, J.D., Sharp, Z.D., Le Brun, M., de Moor, J.M., Barry, P.H., Füri, E., Shaw, A.M., 2015. Temporal variations in fumarole gas chemistry at Poás volcano, Costa Rica. J Volcanol. Geotherm. Res. 294, 56–70.

Frey, F.A., Prinz, M., 1978. Ultramafic inclusions from San Carlos, Arizona: petrologic and geochemical data bearing on their petrogenesis. Earth Planet. Sci. Lett. 38, 129–176.

Frezzotti, M.L., Ferrando, S., 2018. The role of halogens in the lithospheric mantle. In: Harlov, D.E., Aranovich, L. (Eds.), The Role of Halogens in Terrestrial and Extraterrestrial Geochemical Processes. Springer, Cham, pp. 805–845.

Gao, W., Grand, S.P., Baldridge, W.S., Wilson, D., West, M., Ni, J.F., Aster, R., 2004. Upper mantle convection beneath the central Rio Grande rift imaged by P and S wave tomography. J. Geophys. Res. 109, B03305.

Godon, A., Jendrzejewski, N., Castrec-Rouelle, M., Dia, A., Pineau, F., Boulègue, J., Javoy, M., 2004. Origin and evolution of fluids from mud volcanoes in the Barbados accretionary complex. Geochim Cosmochim Acta 68, 2153–2165.

Gregory, R.T., Taylor Jr., H.P., 1981. An oxygen isotope profile in a section of cretaceous oceanic crust, samail ophiolite, Oman: evidence for $\delta^{18}O$ buffering of the oceans by deep (>5 km) seawater-hydrothermal circulation at mid-ocean ridges. J. Geophys. Res. 86 (B4), 2737–2755.

Hacker, B.R., 2008. H_2O subduction beyond arcs. Geochem. Geophys. Geosyst. 9 (3), Q03001.

Hacker, B.R., Abers, G.A., Peacock, S.M., 2003. Subduction factory 1. Theoretical mineralogy, densities, seismic wave speeds, and H_2O contents. J. Geophys. Res. 108 (B1), 2029.

Hanyu, T., Shimizu, K., Ushikubo, T., Kimura, J.-I., Chang, Q., Hamada, M., Ito, M., Iwamori, H., Ishikawa, T., 2019. Tiny droplets of ocean island basalts unveil Earth's deep chlorine cycle. Nature Comm. 10, 60.

Heitmann, E.O., Hyland, E.G., Schoettle-Greene, P., Brigham, C.A.P., Huntington, K.W., 2021. Rise of the Colorado Plateau: a synthesis of paleoelevation constraints from the region and a path forward using temperature-based elevation proxies. Front. Earth Sci. 9, 648605.

Helmstaedt, H., Doig, R., 1975. Eclogite nodules from kimberlite pipes of the Colorado Plateau—Samples of subducted Franciscan-type oceanic lithosphere. Phys. Chem. Earth 9, 95–112.

Herath, P., Stern, T.A., Savage, M.K., Bassett, D., Henrys, S., Boulton, C., 2020. Hydration of the crust and upper mantle of the Hikurangi Plateau as it subducts at the southern Hikurangi margin. Earth Planet. Sci. Lett. 541, 116271.

Hesse, R., Frape, S.K., Egeberg, P.K., Matsumoto, R., 2000. Stable isotope studies (Cl, O, and H) of interstitial waters from Site 997, Blake Ridge has hydrate field, West Atlantic. In: Paull, C.K., Matsumoto, R., Wallace, P.J., Dillon, W.P. (Eds.), Proceedings of the Ocean Drilling Program, Scientific Results 164, 129–137.

Hoare, B.C., Tomlinson, E.L., Barnes, J.D., Tappe, S., Marks, M.A.W., Epp, T., Caulfield, J., Riegler, T., 2021. Tracking halogen recycling and volatile loss in kimberlite magmatism from Greenland: Evidence from combined F-Cl-Br and $\delta^{37}Cl$ systematics. Lithos 384–385, 105976.

Hofmann, A.W., 1997. Mantle geochemistry: the message from oceanic volcanism. Nature 385, 219–229.

Hofmann, A.W., White, W.M., 1982. Mantle plumes from ancient oceanic crust. Earth Planet. Sci. Lett. 57, 421–436.

Hudson, M.R., Grauch, V.J.S., 2013. Introduction. In: Hudson, M.R., Grauch, V.J.S. (Eds.), Geol. Soc. Am. Special Paper 494, 1–20.

Hughes, L., Burgess, R., Chavrit, D., Pawley, A., Tartèse, R., Droop, G., Ballentine, C.J., Lyon, I., 2018. Halogen behaviour in subduction zones: Eclogite facies rocks from the Western and Central Alps. Geochim. Cosmochim. Acta 243, 1–23.

Humphreys, E.D., 1995. Post-Laramide removal of the Farallon slab, western UnitedStates. Geology 23, 987–990.

Humphreys, E., Hessler, E., Dueker, K., Farmer, G.L., Erslev, E., Atwater, T., 2003. How Laramide-age hydration of North American lithosphere by the Farallon Slab controlled subsequent activity in the western United States. Int. Geol. Rev. 45, 575–595.
Jackson, M.G., Koga, K.T., Price, A., Konter, J.G., Koppers, A.A.P., Finlayson, V.A., Konrad, K., Hauri, E.H., Kylander-Clark, A., Kelley, K.A., Kendrick, M.A., 2015. Deeply dredged submarine HIMU glasses from the Tuvalu Islands, Polynesia: Implications for volatile budgets of recycled oceanic crust. Geochem. Geophys. Geosyst. 16, 3210–3234.
John, T., Layne, G.D., Haase, K.M., Barnes, J.D., 2010. Chlorine isotope evidence for crustal recycling into the Earth's mantle. Earth Planet. Sci. Lett. 298, 175–182.
John, T., Scambelluri, M., Frische, M., Barnes, J.D., Bach, W., 2011. Dehydration of subducting serpentinite: implications for halogen mobility in subduction zones and the deep halogen cycle. Earth Planet. Sci. Lett. 308, 65–76.
Karlstrom, K.E., Bowring, S.A., 1993. Proterozoic orogenic history of Arizona. In: Reed, J. C. (Ed.) Precambrian, conterminous U.S.: Boulder, Colorado, Geological Society of America, Geology of North America C-2, pp. 189–211.
Kendrick, M.A., 2019a. Halogens in Atlantis Bank gabbros, SW Indian Ridge: Implications for styles of seafloor alteration. Earth Planet. Sci. Lett. 514, 96–107.
Kendrick, M.A., 2019b. Halogens in altered ocean crust from the East Pacific Rise (ODP/IODP Hole 1256D). Geochim. Cosmocim. Acta 261, 93–112.
Kendrick, M.A., Hémond, C., Kamenetsky, V.S., Danyushevsky, L., Devey, C.W., Rodermann, T., Jackson, M.G., Perfit, M.R., 2017. Seawater cycled throughout Earth's mantle in partially serpentinized lithosphere. Nature Geosci. 10, 222–227.
Klemme, S., Stalder, R., 2018. Halogens in the Earth's Mantle: What We Know and What We Don't. In: Harlov, D.E., Aranovich, L. (Eds.), The Role of Halogens in Terrestrial and Extraterrestrial Geochemical Processes. Springer, Cham, pp. 847–869.
Lassiter, J.C., Hauri, E.H., Nikogosian, I.K., Barsczus, H.G., 2002. Chlorine-potassium variations in melt inclusions from Raivavae and Rapa, Austral Islands: constraints on chlorine recycling in the mantle and evidence for brine-induced melting of oceanic crust. Earth Planet. Sci. Lett. 202, 525–540.
Lawton, T.F., McMillan, N.J., 1999. Arc abandonment as a cause for passive continental rifting: comparison of the Jurassic Mexican Borderland rift and the Cenozoic Rio Grande rift. Geology 27, 779–782.
Layne, G.D., Kent, A.J.R., Bach, W., 2009. δ37Cl systematics of a backarc spreading system: the Lau Basin. Geol. 37 (5), 427–430.
le Roux, P.J., Shirey, S.B., Hauri, E.H., Perfit, M.R., Bender, J.F., 2006. The effects of variable sources, processes and contaminants on the composition of northern EPR MORB (8–10°N and 12–14°N): Evidence from volatiles (H2O, CO2, S) and halogens (F, Cl). Earth Planet. Sci. Lett. 251, 209–231.
Le Voyer, M., Cottrell, E., Kelley, K.A., Brounce, M., Hauri, E.H., 2015. The effect of primary versus secondary processes on the volatile content of MORB glasses: an example from the equatorial Mid-Atlantic Ridge (5°N–3°S). J. Geophys. Res. 120, 125–144.
Lee, C.-T.-A., 2005. Trace element evidence for hydrous metasomatism at the base of the North American lithosphere and possible association with Laramide low-angle subduction. J. Geol. 113, 673–685.
Lee, C.-T.-A., Yin, Q., Rudnick, R.L., Jacobsen, S.B., 2001. Preservation of ancient and fertile lithospheric mantle beneath the southwestern United States. Nature 411, 69–72.
Lesne, P., Kohn, S.C., Blundy, J., Witham, F., Botcharnikov, R.E., Behrens, H., 2011. Experimental Simulation of Closed-System Degassing in the System Basalt-H_2O-CO_2-S-Cl. J. Petrol. 52 (9), 1737–1762.
Li, Z.X.A., Lee, C.T.A., Peslier, A.H., Lenardic, A., Mackwell, S.J., 2008. Water contents in mantle xenoliths from the Colorado Plateau and vicinity: implications for the mantle rheology and hydration-induced thinning of continental lithosphere. J. Geophys. Res. 113 (B9), B09210.
Liebscher, A., Barnes, J.D., Sharp, Z.D., 2006. Chlorine isotope vapor-liquid fractionation during experimental fluid-phase separation at 400°C/23 MPa to 450°C/42 MPa. Chem. Geol. 234, 340–345.
Liotta, M., Rizzo, A.L., Barnes, J.D., D'Auria, L., Martelli, M., Bobrowski, N., Wittmer, J., 2017. Chlorine Isotope Composition of Volcanic Rocks and Gases at Stromboli Volcano (Aeolian Islands, Italy): inferences on Magmatic Degassing Prior to 2014 Eruption. J. Volcanol. Geothermal Res. 336, 168–178.
Liu, S., Currie, C.A., 2016. Farallon plate dynamics prior to the Laramide orogeny: numerical models of flat subduction. Tectonophys. 666, 33–47.
Liu, L., Spasojević, S., Gurnis, M., 2008. Farallon plate dynamics prior to the Laramide orogeny: numerical models of flat subduction. Science 322, 934–938.
Livaccari, R.F., Burke, K., Sengör, A.M.C., 1981. Was the Laramide orogeny related to subduction of an oceanic plateau? Nature 289, 276–278.
Mack, G.H., Nightengale, A.L., Seager, W.R., Clemons, R.E., 1994. The Oligocene Goodsight-Cedar Hills half graben near Las Cruces and its implications to the evolution of the Mogollon-Datil volcanic field and to the southern Rio Grande rift. New Mex. Geol. Soc. Guidebook 45, 135–142.
Magenheim, A.J., Spivack, A.J., Volpe, C., Ransom, B., 1994. Precise determination of stable chlorine isotopic ratios in low-concentration natural samples. Geochim. Cosmochim. Acta 58 (14), 3117–3121.
Manzini, M., Bouvier, A.-S., Barnes, J.D., Bonifacie, M., Rose-Koga, E.F., Ulmer, P., Métrich, N., Bardoux, G., Williams, J., Layne, G.D., Straub, S., Baumgartner, L.P., John, T., 2017. SIMS chlorine isotope analyses in melt inclusions from arc settings. Chem. Geol. 449, 112–122.
Marshall, E.W., Lassiter, J.C., Barnes, J.D., Luguet, A., Lissner, M., 2017a. Mantle melt production during the 1.4 Ga Laurentian magmatic event: Isotopic constraints from Colorado Plateau mantle xenoliths. Geology 45 (6), 519–522.
Marshall, E.W., Barnes, J.D., Lassiter, J.C., 2017b. The role of serpentinite-derived fluids in metasomatism of the Colorado Plateau (USA) lithospheric mantle. Geology 45 (12), 1–4.
Marshall, E., Lassiter, J.C., Barnes, J.D., 2018. On the (mis)behavior of water in the mantle: controls on nominally anhydrous mineral water contents in mantle peridotites. Earth Planet. Sci. Lett. 499, 219–229.
Mattey, D., Lowry, D., Macpherson, C., 1994. Oxygen isotope composition of mantle peridotite. Earth Planet. Sci. Lett. 128, 231–241.
McGetchin, T.R., Nikhanj, Y.S., Chodos, A.A., 1973. Carbonatite-kimberlite relations in the Cane Valley diatreme, San Juan County, Utah. J. Geophys. Res. 78, 1854–1869.
McMillan, N.J., Dickin, A.P., Haag, D., 2000. Evolution of magma source regions in the Rio Grande rift, southern New Mexico. GSA Bull. 112 (10), 1582–1593.
Pagé, L., Hattori, K., de Hoog, J.C.M., Okay, A.I., 2016. Halogen (F, Cl, Br, I) behaviour in subducting slabs: a study of lawsonite blueschists in western Turkey. Earth Planet. Sci. Lett. 44, 133–142.
Perkins, G.B., Sharp, Z.D., Selverstone, J., 2006. Oxygen isotope evidence for subduction and rift- related mantle metasomatism beneath the Colorado Plateau-Rio Grande rift transition. Contrib. Mineral. Petrol. 151, 633–650.
Philippot, P., Agrinier, P., Scambelluri, M., 1998. Chlorine cycling during subduction of altered oceanic crust. Earth Planet. Sci. Lett. 161, 33–44.
Ransom, B., Spivack, A.J., Kastner, M., 1995. Stable Cl isotopes in subduction-zone pore waters: Implications for fluid–rock reactions and the cycling of chlorine. Geology 23, 715–718.
Roden, M., 1981. Origin of coexisting minette and ultramafic breccia, Navajo volcanic field. Contrib. Mineral. Petrol. 77, 195–206.
Roden, M., Shimizu, N., 1993. Ion microprobe analyses bearing on the composition of the upper mantle beneath the Basin and Range and Colorado Plateau provinces. J. Geol. Res. 98 (93), 14091–14108.
Roden, M.F., Smith, D., Murthy, V.R., 1990. Chemical constraints on lithosphere composition and evolution beneath the Colorado Plateau. J. Geophys. Res. 95, 2811–2831.
Rowe, M.C., Lassiter, J.C., 2009. Chlorine enrichment in central Rio Grande Rift basaltic melt inclusions: Evidence for subduction modification of the lithospheric mantle. Geology 37 (5), 439–442.
Rowe, M.C., Lassiter, J.C., Goff, K., 2015. Basalt volatile fluctuations during continental rifting: An example from the Rio Grande Rift, USA. Geochem. Geophys. Geosyst. 16, 1254–1273.
Saal, A.E., Hauri, E.H., Langmuir, C.H., Perfit, M.R., 2002. Vapour undersaturation in primitive mid-ocean-ridge basalt and the volatile content of the Earth's upper mantle. Nature 419, 451–455.
Saccocia, P.J., Seewald, J.S., Shanks, W.C.I.I.I., 2009. Oxygen and hydrogen isotope fractionation in serpentine–water and talc–water systems from 250 to 450°C, 50 MPa. Geochim. Cosmochim. Acta 73, 6789–6804.
Schauble, E.A., Rossman, G.R., Taylor Jr., H.P., 2003. Theoretical estimates of equilibrium chlorine-isotope fractionations. Geochim. Cosmochim. Acta 67 (17), 3267–3281.
Schmidt, M.W., Poli, S., 1998a. Experimentally based water budgets for dehydrating slabs and consequences for arc magma generation. Earth Planet. Sci. Lett. 163, 361–379.
Schmidt, M.W., Poli, S., 1998b. Experimentally based water budgets for dehydrating slabs and consequences for arc magma generation. Earth Planet. Sci. Lett. 163, 361–379.
Segee-Wright, G., Barnes, J.D., Lassiter, J.C., Holmes, D.J., Beaudoin, G.M., Chatterjee, R., Stockli, D.F., Hoffmann, J.E., John, T., 2023. Halogen enrichment in the North American lithospheric mantle from the dehydration of the Farallon plate. Geochim. Cosmochim. Acta 348, 187–205.
Selverstone, J., Pun, A., Condie, K.C., 1999. Xenolithic evidence for Proterozoic crustal evolution beneath the Colorado Plateau. GSA Bulletin 111 (4), 590–606.
Selverstone, J., Sharp, Z.D., 2011. Chlorine isotope evidence for multicomponent mantle metasomatism in the Ivrea Zone. Earth Planet. Sci. Lett. 310, 429–440.
Selverstone, J., Sharp, Z.D., 2015. Chlorine isotope behavior during prograde metamorphism of sedimentary rocks. Earth Planet. Sci. Lett. 417, 120–131.
Sharp, Z.D., Atudorei, V., Durakiewicz, T., 2001. A rapid method for determination of hydrogen and oxygen isotope ratios from water and hydrous minerals. Chem. Geol. 178, 197–210.
Sharp, Z.D., Barnes, J.D., Brearley, A.J., Chaussidon, M., Fischer, T.P., Kamenetsky, V.S., 2007. Chlorine isotope homogeneity of the mantle, crust, and carbonaceous chondrites. Nature 446, 1062–1065.
Sharp, Z.D., Barnes, J.D., Fischer, T.P., Halick, M., 2010. A laboratory determination of chlorine isotope fractionation in acid systems and applications to volcanic fumaroles. Geochim. Cosmochim. Acta 74, 264–273.
Sharp, Z.D., Draper, D.S., 2013. The chlorine abundance of Earth: Implications for a habitable planet. Earth Planet. Sci. Lett. 369, 71–77.
Sharp, Z.D., Mercer, J.A., Jones, R.H., Brearley, A.J., Selverstone, J., Bekker, A., Stachel, T., 2013. The chlorine isotope composition of chondrites and Earth. Geochim. Cosmochim. Acta 107, 189–204.
Shaw, A.M., Hauri, E.H., Fischer, T.P., Hilton, D.R., Kelley, K.A., 2008. Hydrogen isotopes in Mariana arc melt inclusions: Implications for subduction dehydration and the deep-Earth water cycle. Earth Planet. Sci. Lett. 275, 138–145.
Shirey, S.B., Wagner, L.S., Walters, M.J., Pearson, D.G., van Keken, P.E., 2021. Slab Transport of fluids to deep focus earthquake depths—Thermal modeling constraints and evidence from diamonds. AGU Adv. 2.
Smith, D., 1979. Hydrous minerals and carbonates in peridotite inclusions from Green Knobs and Buell Park kimberlitic diatremes on the Colorado Plateau. In: Boyd, F.R., Meyer, H.O.A. (Eds.), The Mantle Sample: Inclusions in Kimberlites and Other Volcanics. American Geophysical Union, Washington D.C., pp. 345–356

Smith, D., 1995. Chlorite-rich ultramafic reaction zones in Colorado Plateau xenoliths: recorders of sub-Moho hydration. Contrib. Mineral. Petrol. 121, 185–200.
Smith, D., 2010. Antigorite peridotite, metaserpentinite, and other inclusions within diatremes on the Colorado Plateau, SW USA: implications for the mantle wedge during low-angle subduction. J. Pet. 51, 1355–1379.
Smith, D., 2013. Olivine thermometry and source constraints for mantle fragments in the Navajo Volcanic Field, Colorado Plateau, southwest United States: implications for the mantle wedge. Geochem. Geophys. Geosyst. 14, 693–711.
Smith, D., 2020. Trace elements in Cr-pyrope from the Navajo volcanic field of the Colorado Plateau, SW USA, and implications for the mantle wedge during low-angle subduction. Lithos 362–363, 105460.
Smith, D., Griffin, W.L., 2005. Garnetite xenoliths and mantle-water interactions below the Colorado Plateau, Southwestern United States. J. Petrol. 46 (9), 1901–1924.
Smith, D., Levy, S., 1976. Petrology of the Green Knobs diatreme and implications for the upper mantle below the Colorado Plateau. Earth Planet. Sci. Lett. 29, 107–125.
Smith, D., Connelly, J.N., Manser, K., Moser, D.E., Housh, T.B., McDowell, F.W., Mack, L. E., 2004. Evolution of Navajo eclogites and hydration of the mantle wedge below the Colorado Plateau, southwestern United States. Geochem. Geophys. Geosyst. 5 (4), Q04005.
Spandler, C., Hermann, J., 2006. High-pressure veins in eclogite from New Caledonia and their significance for fluid migration in subduction zones. Lithos 89 (1–2), 135–153.
Spandler, C., Pettke, T., Rubatto, D., 2011. Internal and External Fluid Sources for Eclogite-facies Veins in the Monviso Meta-ophiolite, Western Alps: implications for fluid flow in subduction zones. J. Petrol. 52 (6), 1207–1236.
Stroncik, N.A., Haase, K.M., 2004. Chlorine in oceanic intraplate basalts: constraints on mantle sources and recycling processes. Geology 32 (11), 945–948.
Syracuse, E.M., van Keken, P.E., Abers, G.A., 2010. The global range of subduction zone thermal models. Phys. Earth Planet. Int. 183, 73–90.
Unni, C.K., Schilling, J.G., 1978. Cl and Br degassing by volcanism along the Reykjanes Ridge and Iceland. Nature 272, 19–23.
Urann, B.M., Le Roux, V., John, T., Beaudoin, G.M., Barnes, J.D., 2020. The distribution and abundance of halogens in eclogites: An in-situ SIMS perspective of the Raspas Complex (Ecuador). Am. Mineral. 105, 307–318.
Usui, T., Nakamura, E., Kobayashi, K., Maruyama, S., Helmstaedt, H., 2003. Fate of the subducted Farallon plate inferred from eclogite xenoliths in the Colorado Plateau. Geology 31 (7), 589–592.
Valley, J.W., Kitchen, N., Kohn, M.J., Niendorf, C.R., Spicuzza, M.J., 1995. UWG-2, a garnet standard for oxygen isotope ratios: Strategies for high precision and accuracy with laser heating. Geochim. Cosmochim. Acta 59, 5223–5231.
van Keken, P.E., Hacker, B.R., Syracuse, E.M., Abers, G.A., 2011. Subduction factory: 4. Depth-dependent flux of H_2O from subducting slabs worldwide. J. Geophys. Res. Solid Earth 116 (B1).
Weiss, Y., McNeill, J., Pearson, D.G., Nowell, G.M., Ottley, C.J., 2015. Highly saline fluids from a subducting slab as the source for fluid-rich diamonds. Nature 524, 339–342.
West, M., Ni, J., Baldridge, W.S., Wilson, D., Aster, R., Gao, W., Grand, S., 2004. Crust and upper mantle shear wave structure of the southwest United States: implications for rifting and support for high elevation. J. Geophys. Res. 109, B03309.
Whitney, D.L., Fornash, K.F., Kang, P., Ghent, E.D., Martin, L., Okay, A.I., Brovarone, A. V., 2020. Lawsonite composition and zoning as tracers of subduction processes: a global review. Lithos 370–371, 105636.
Wilson, D., Aster, R., West, M., Ni, J., Grand, S., Gao, W., Baldridge, W.S., Semken, S., Patel, P., 2005. Lithospheric structure of the Rio Grande rift. Nature 433, 851–855.